Jambura Journal of Biomathematics

RESEARCH ARTICLE

Mathematical Modeling of COVID-19: An Optimal Control Approach

Ayodeji Sunday Afolabi[1,✉] **and Abdulwahab Ridwan**[1]

[1]Department of Mathematical Sciences, Federal University of Technology, Akure, P.M.B. 704, Akure, Ondo State, Nigeria

✉Corresponding author. Email: *asafolabi@futa.edu.ng*

Article Identity
Jambura J. Biomath.
Volume 7 Issue 1 Pages 1 – 27
March 2026, E-ISSN 2723-0317

Article History
Received 19 April 2025
Revised 9 January 2026
Accepted 27 January 2026
Published 17 March 2026

Keywords
COVID-19, Non-linear, Stability analysis, Objective functional, Hamiltonian function, Optimal control problem

Editorial office: Department of Mathematics, Universitas Negeri Gorontalo, Jln. Prof. Dr. Ing. B. J. Habibie, Bone Bolango 96554, Indonesia

To Cite this Article: Afolabi AS and Ridwan A. Mathematical Modeling of COVID-19: An Optimal Control Approach. Jambura Journal of Biomathematics. 2026;7(1):1-27. doi:10.37905/jjbm.v7i1.2

Abstract. *A non-linear mathematical model is developed to describe the transmission dynamics of COVID-19. The model's well-posedness is verified by analyzing the positivity and boundedness of its solutions. Analytical expressions for the disease-free equilibrium points are derived and the stability analyses of the disease-free and endemic equilibrium points are conducted. A sensitivity analysis of the model parameters with respect to the basic reproduction number* (R_0) *is carried out to identify the key factors influencing COVID-19 transmission. Consequently, the model is extended into an optimal control problem by incorporating three time-dependent interventions: preventive measures (such as travel restrictions and personal protection), continuous vaccination of susceptible individuals, and testing, isolation, and treatment of infected cases. Four control strategies, each combining at least two interventions, are explored. The autonomous and non-autonomous systems are analyzed. Numerical simulations indicate that implementing the three control measures concurrently provides the most effective strategy to mitigating the spread of COVID-19.*

1. Introduction

COVID-19 is an infectious disease caused by the SARS-CoV-2 virus, which can result in severe acute respiratory syndrome (SARS). Some of the common symptoms of COVID-19 include cough, fatigue, fever, and a loss of taste and smell. Others are body aches, headaches, persistent dry coughing, intense chest pain, elevated temperature, and respiratory system complications are some of the symptoms of the disease. The disease can be transmitted through respiratory droplets, most commonly when coughing or sneezing. COVID-19 was first reported in Wuhan, China, in 2019, the novel human coronavirus 2019 (COVID-19) quickly spread throughout the world. Although a greater incubation duration of 25 days has also been documented, the COVID-19 incubation period typically lasts between 0 and 14 days. The ratio of the death rate is lower than its recovery rate and fluctuates from nation to nation and region to region [1].

There are multiple approaches to preventing the spread of COVID-19. The best practice among them includes social distancing and self-quarantine. Scholars worldwide are concentrating their efforts on providing some practical solutions to combat the pandemic. Getting vaccinated is a good preventative measure against infectious diseases. To reduce the global incidence of COVID-19 infection, vaccination is crucial, as is the stringent application of non-pharmaceutical therapies [1, 2].

The first case of COVID-19 was confirmed in Nigeria on February 27, 2020, signaling the arrival

of the pandemic in the country. Throughout the period of the outbreak of the disease in Nigeria, the response efforts to mitigate the spread of COVID-19 were spearheaded by National Emergency Operations Center (EOC) within the Nigeria Centre for Disease Control (NCDC). This central command closely collaborates with the State Public Health Emergency Operations Centres, fostering a coordinated approach across different regions of the nation [1–4].

The global COVID-19 situation experienced a resurgence in cases even as deaths declined between July 10 and August 6, 2023. About 1.5 million new cases were reported worldwide during this 28-day span, marking an 80% spike compared to the prior 28 days. However, the death toll showed a 57% decrease, with over 2,500 new fatalities recorded. While five of the World Health Organization's regions witnessed drops in both cases and deaths, the Western Pacific stood out by registering an uptick in case numbers alongside a downward trend in mortality [5].

The latest epidemiological update from the World Health Organization shows encouraging signs regarding the COVID-19 pandemic, though challenges persist. From February 5 to March 3, 2024, reported global cases and deaths declined substantially compared to the previous 28-day period. The SARS-CoV-2 variant JN.1 emerged as the predominant strain, comprising over 90% of sequenced cases, while its parent lineage BA.2.86 waned. Hospitalizations and intensive care unit admissions among reporting countries also saw notable decreases of 34% and 61%, respectively. However, dwindling COVID-19 testing and genomic surveillance efforts worldwide have made comprehensive evaluation the pandemic's trajectory increasingly difficult. While severity indicators like the proportion of hospitalizations requiring ICU care or resulting in death have been improving, the reasons likely stem from a number of factors including greater population immunity and enhancements to clinical care capabilities. Nonetheless, gaps in monitoring underscore the persisting threats posed by COVID-19 [5].

Many researchers have developed mathematical models in order to understand and investigate the complex structure of the pandemic, and make useful recommendations that will help to contain the disease [4, 6–58]. [1] proposed an optimal control problem (OCP) for combatting COVID-19 pandemic with four control measures: management control, detection control, personal protection, and contact tracing and testing. The results indicated that combining all the four control measures at the optimal levels is the most effective measure to reduce the disease burden [1]. [44] analyzed an SEIRW COVID-19 model with respect to the continuous threat posed by the disease and the need for efficient disease containment measures. The equilibria obtained from the model were examined by conducting local and global stability assessments, providing important insights into the disease transmission dynamics. The efficacy of suggested control strategies was evaluated through the application of Pontryagin's maximal principle (PMP) and numerical simulations. [45] assessed the effectiveness of non-pharmacological control strategies in combating the COVID-19 pandemic. The implementation of two interventions showed some positive effects in combating the disease. In addition, the results indicated that the implementation of all the three strategies lowered the threshold of the disease, although complete eradication of the virus was not achieved.

[46] employed the use of PMP to apply optimal and sub-optimal controls to SEQIJR SARS model. The model takes into account two control variables that stand in for the isolation and quarantine tactics. The outcomes of the numerical simulation showed that, in both optimal and sub-optimal control scenarios, the early stages of the epidemic were crucial for the maximum implementation of isolation and quarantine protocols. [47] developed an optimal control model to study the transmission dynamics of COVID-19 and the important properties of the model, such as non-negativity, boundedness of solutions, and the region of invariance were established. The significance of treatment, hand sanitizers, and face masks as control measures in the management of the disease were examined. The results indicated that efficient control strategies could lower the fundamental reproduction number (R_0), which could lead to the eradication of the disease when it is below unity. Based on the information from the Nigeria Center for Disease Control (NCDC), the study emphasized the importance of

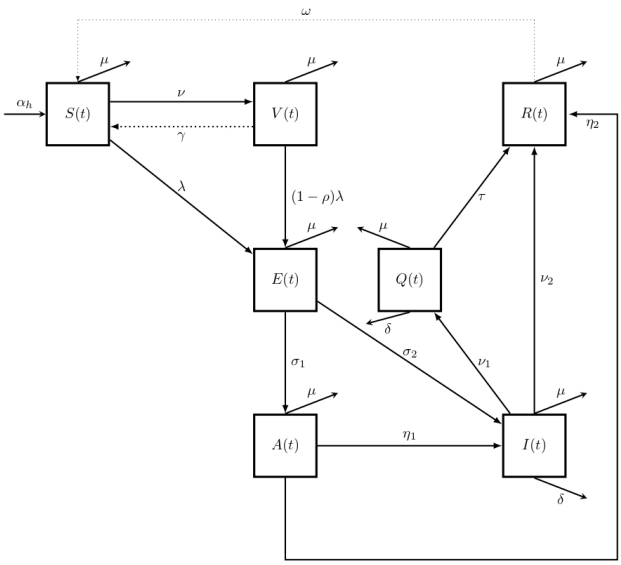

Figure 1. Flowchart of the model

legislators and government agencies to put these policies in place and keep them up to date in order to effectively fight COVID-19 in Nigeria [2]. [48] proposed a deterministic compartmental model for the study of the transmission dynamics of the third wave of COVID-19 pandemic in Nigeria, incorporating optimal control measures. The study offered insights for future epidemic preparedness by assessing the impacts of the control variables on the disease transmission. The model was further developed into an OCP and analyzed through PMP. The theoretical results were validated through numerical solutions, applying COVID-19 data from Nigeria. These results further showed the significant impacts of these measures on reducing the disease spread, emphasizing the importance of their proper implementation for successful disease control.

A COVID-19 model incorporating optimal control measures in the presence of vaccination was formulated. The scenario without vaccination was also considered and the stability analyses for the two scenarios were examined. Four control measures were proposed. An optimal control model was developed based on these measures, and some mathematical results were obtained. The effectiveness of optimal controls in reducing the number of infected individuals and improving population health were demonstrated from the numerical simulations [38]. [49] presented a model for the dynamics of COVID-19 pandemic and examined the effectiveness of vaccination in curtailing the disease. Various vaccine efficacy levels were considered and the control measure scenarios were investigated through numerical simulations. To achieve these results, optimal control theory was employed to obtain the important optimality requirements. [50] proposed a SEIAPHR model to understand the dynamics of COVID-19. This model classified infected individuals into three categories and they employed optimal control approach to assess the effectiveness of the control strategies, demonstrating numerically that these strategies can drastically reduce new infections. [51] developed a mathematical model for the control of COVID-19, incorporating some control measures into the model. The findings revealed that the controlled system had a significant impact when compared to situations without control.

The importance of World Health Organization's vigilance in containing COVID-19 variants and the necessity for predictive decision-making in allocating resources for public welfare are highlighted. An efficiency analysis to derive an optimal control approach for curtailing COVID-19 transmission in Akwa Ibom state, Nigeria was presented employing a deterministic epidemic model with three time-varying control functionals: educational programs, vaccination, and treatment. An optimality system, derived from PMP, was employed for the assessment, with forward-backward numerical so-

lutions calculated using validated datasets from NCDC. The efficiency analysis identified Strategy I, a combination of educational intervention and vaccination, as the most efficacious, with a 96% reduction in the infected sub-population was considered [3]. [52] formulated a mathematical model that described the transmission dynamics of COVID-19, considering various population groups and their interactions. An optimal strategy aimed at reducing virus transmission through awareness campaigns, airport surveillance, and quarantine measures was incorporated into the model. The optimal controls were determined by applying the necessary conditions of optimality on the optimal control model. The results of the numerical simulations agreed favourably well with the theoretical findings. [53] investigated population-wide policies to tackle the COVID-19 pandemic in India, highlighting the urgent need for intervention. An SAIQJR model that incorporated various stages of infection, allowing them to assess the pandemic's progression and control strategies was proposed and analyzed. Optimal control measures that combined pharmaceutical and non-pharmaceutical interventions, aiming to reduce disease fatality and new infections were explored. The results from the numerical simulations revealed the effectiveness of intervention strategies, particularly the combined application of the controls, in controlling the transmission dynamics of COVID-19. [54] investigated the influence of media coverage on the spread and control of COVID-19 through a comprehensive mathematical model. The study revealed that effective management of quarantine and medical care could help to curb disease prevalence. [55] opined that many barriers could affect effective management efforts due to the limitations and problems associated with controlling COVID-19. These comprised variations in vaccination rates, vaccine apprehension, unequal access to care, the appearance of novel variations, pandemic exhaustion, international connectedness and travel, and pressure on healthcare systems. To tackle these obstacles, comprehensive approaches were needed, taking into account public health messaging, socioeconomic variables, and the use of mathematical modeling to direct interventions.

This study addresses the gaps by formulating a nonlinear seven compartmental optimal control model that evaluates four integrated intervention strategies, each combining at least two of three time-dependent controls, to determine the most effective approach for COVID-19 mitigation in Nigeria. Its key contribution is a direct comparison of the triple-control strategy with three pairwise strategies using Nigeria-specific parameters, offering evidence-based insights for optimal public health decision-making.

2. Model Formulation

The total human population is divided into seven distinct groups: Susceptible (S), Vaccinated (V), Exposed (E), Asymptomatic (A), Infected (I), Quarantined (Q), and Recovered (R). The force of infection is defined as

$$\lambda(t) = \beta_1 E + \beta_2 A + \beta_3 I + \beta_4 Q$$

The parameters $\beta_i, I = 1,2,3,4$ are as defined in Table 1. The flowchart for the proposed model's population dynamics is shown in Figure 1.
The proposed COVID-19 model is described as:

$$\begin{aligned}
\frac{dS}{dt} &= \alpha + \gamma V + \omega R - \lambda S - \nu S - \mu S,\\
\frac{dV}{dt} &= \nu S - (1-\rho)\lambda V - \gamma V - \mu V,\\
\frac{dE}{dt} &= \lambda S + (1-\rho)\lambda V - \sigma_1 E - \sigma_2 E - \mu E,\\
\frac{dA}{dt} &= \sigma_1 E - \eta_1 A - \eta_2 A - \mu A,\\
\frac{dI}{dt} &= \sigma_2 E + \eta_1 A - \nu_1 I - \nu_2 I - \delta I - \mu I,
\end{aligned} \tag{1}$$

$$\frac{dQ}{dt} = \nu_1 I - \tau Q - \delta Q - \mu Q,$$
$$\frac{dR}{dt} = \eta_2 A + \nu_2 I + \tau Q - \omega R - \mu R,$$

with the initial conditions

$$S(0) > 0, V(0) \geq 0, E(0) \geq 0, A(0) \geq 0, I(0) \geq 0, Q(0) \geq 0, R(0) \geq 0. \tag{2}$$

Table 1. Model parameters and descriptions

Parameter	Description
α	Recruitment rate
μ	Natural death rate
δ	Disease-induced death rate
ω	Rate of waning immunity
β_1	Transmission rate from $E(t)$
β_2	Transmission rate from $A(t)$
β_3	Transmission rate from $I(t)$
β_4	Transmission rate from $Q(t)$
ρ	Vaccine efficacy
ν	Vaccination rate of $S(t)$
γ	Loss of vaccine-induced immunity rate
σ_1	Progression rate from $E(t)$ to $A(t)$
σ_2	Progression rate from $E(t)$ to $I(t)$
η_1	Progression rate from $A(t)$ to $I(t)$
η_2	Recovery rate of $A(t)$
ν_1	Quarantine rate of $I(t)$
ν_2	Recovery rate of $I(t)$
τ	Recovery rate of $Q(t)$

3. Analytical Results

3.1. The invariant region and positivity of solutions

Theorem 1. *The region of system (1) defined by the set $\Omega(t)$ is positively invariant with $\Omega(t) \geq 0 \in \mathbb{R}^7_+$.*

Proof. The total population is defined as

$$N = S + V + E + A + I + Q + R.$$

Thus,

$$\frac{dN}{dt} = \frac{dS}{dt} + \frac{dV}{dt} + \frac{dE}{dt} + \frac{dA}{dt} + \frac{dI}{dt} + \frac{dQ}{dt} + \frac{dR}{dt}.$$

Hence,

$$\frac{dN}{dt} \leq \alpha - \mu N.$$

The solution satisfies

$$(\alpha - \mu N) \geq Ae^{-\mu t},$$

where A is the integration constant. Let $N(0) = N_0$. Then,

$$(\alpha - \mu N_0) \geq A.$$

Thus,

$$N(t) \leq \frac{\alpha}{\mu} - \left(\frac{\alpha}{\mu} - N_0\right) e^{-\mu t}.$$

Hence,

$$N(t) \in \left[0, \frac{\alpha}{\mu}\right].$$

Therefore, the invariant region containing the solutions of system (1) is given by

$$\Omega = \{(S(t), V(t), E(t), A(t), I(t), Q(t), R(t)) \in \mathbb{R}_+^7 : N(t) \leq \tfrac{\alpha}{\mu}\}.$$

■

Theorem 2. *If the initial values $S(0) \geq 0$, $V(0) \geq 0$, $E(0) \geq 0$, $A(0) \geq 0$, $I(0) \geq 0$, $Q(0) \geq 0$, $R(0) \geq 0$ for all $t > 0$, then the solution $(S(t), V(t), E(t), A(t), I(t), Q(t), R(t))$ of the system (1) is positively invariant.*

Proof. Assume that

$$\hat{t} = \sup\{S(0) \geq 0, V(0) \geq 0, E(0) \geq 0, A(0) \geq 0, I(0) \geq 0, Q(0) \geq 0, R(0) \geq 0\},$$

this implies that $\hat{t} > 0$,

$$S(t) \geq S(0) e^{\left(-(\nu+\mu)t - \int_0^t \lambda(\eta) d\eta\right)} \geq 0, \quad \forall t \geq 0.$$

where $\lambda(\eta) = \beta_1 E(\eta) + \beta_2 A(\eta) + \beta_3 I(\eta) + \beta_4 Q(\eta)$. Similarly,

$$\begin{aligned}
V(t) &\geq V(0) e^{-((\gamma+\mu)t - (1-\rho)\int_0^t \lambda(\eta) d\eta)}, \\
E(t) &\geq E(0) e^{-((\sigma_1+\sigma_2+\mu)t)}, \\
A(t) &\geq A(0) e^{-((\eta_1+\eta_2+\mu)t)}, \\
I(t) &\geq I(0) e^{-((\nu_1+\nu_2+\delta+\mu)t)}, \\
Q(t) &\geq Q(0) e^{-((\tau+\delta+\mu)t)}, \\
R(t) &\geq R(0) e^{-((\omega+\mu)t)}.
\end{aligned}$$

Thus, $\forall t > 0$, all variables of the model are positive. ■

The invariant region and positivity of solutions ensure that every state variable remains non-negative and bounded $\forall t > 0$ which is essential since population compartments represent real biological quantities that cannot be negative or unbounded. Biologically, this guarantees that the model dynamics are epidemiologically meaningful and that conclusions such as stability and persistence correspond to feasible disease behavior in the population.

3.2. Existence of equlibria

1. the disease free equilibrium point (DFE):
   There are no infections at the DFE. Therefore, the number of infected individuals at this point is zero. Thus, the DFE is obtained as

$$\mathscr{E}^0 = \left(S^0 = \frac{\alpha(\mu+\gamma)}{(\mu+\nu)(\mu+\gamma) - \nu\gamma},\ V^0 = \frac{\nu\alpha}{(\mu+\nu)(\mu+\gamma) - \nu\gamma},\ E^0 = 0,\ A^0 = 0,\ I^0 = 0,\ Q^0 = 0,\ R^0 = 0.\right).$$

2. the basic reproduction number
From the Diekmann-Heesterbeek-Metz Next Generation Matrix approach, the basic reproduction number is defined as FV^{-1} for system (1) [6–9]. This implies that

$$F = \begin{pmatrix} \beta_1 S^0 & \beta_2 S^0 & \beta_3 S^0 & \beta_4 S^0 \\ 0 & 0 & 0 & 0 \\ 0 & 0 & 0 & 0 \\ 0 & 0 & 0 & 0 \end{pmatrix},$$

$$V = \begin{pmatrix} k_3 & 0 & 0 & 0 \\ -\sigma_1 & k_4 & 0 & 0 \\ -\sigma_2 & -\eta_1 & k_5 & 0 \\ 0 & 0 & -\nu_1 & k_6 \end{pmatrix}.$$

where

$$k_1 = \nu + \mu, \quad k_2 = \gamma + \mu, \quad k_3 = \sigma_1 + \sigma_2 + \mu, \quad k_4 = \eta_1 + \eta_2 + \mu,$$
$$k_5 = \nu_1 + \nu_2 + \delta + \mu, \quad k_6 = \tau + \delta + \mu, \quad k_7 = \omega + \mu.$$

Thus, R_0 is defined as:

$$\mathbb{R}_0 = \frac{\alpha k_2}{(k_1 k_2 - \nu\gamma) k_3 k_4 k_5 k_6} \Big(\beta_1 k_4 k_5 k_6 + \beta_2 \sigma_1 k_5 k_6 + \beta_3 (\eta_1 \sigma_1 k_6 + k_4 \sigma_2 k_6) + \beta_4 (\eta_1 \nu_1 \sigma_1 + k_4 \nu_1 \sigma_2) \Big).$$

$\mathbb{R}_0$ is influenced by several epidemiological contributions. The constant term αk_2 in the numerator represents the recruitment of new susceptible individuals. The terms $\beta_1 k_4 k_5 k_6$ and $\beta_2 k_5 k_6 \sigma_1$ correspond to disease transmission from exposed and asymptomatic individuals, respectively. Transmission from symptomatic infected individuals is captured by the terms $\beta_3 \eta_1 k_6 \sigma_1$ and $\beta_3 k_4 k_6 \sigma_2$, while the contributions $\beta_4 \eta_1 \nu_1 \sigma_1$ and $\beta_4 k_4 \nu_1 \sigma_2$ account for infection arising from quarantined individuals. Collectively, these terms increase the potential for disease spread whereas the denominator of R_0 incorporates removal and progression rates that act to reduce the overall transmission potential.

3. stability of disease-free equilibrium point

Theorem 3. *The disease-free equilibrium point is locally asymptotically stable provided* $\mathbb{R}_0 < 1$ *and unstable otherwise.*

Proof. Let $\mathscr{E}^0$ denote the DFE of system (1). At this point, there are no exposed or infectious individuals, so $E = A = I = Q = 0$. The Jacobian matrix of system (1) evaluated at $\mathscr{E}^0$ can be written as

$$J(\mathscr{E}^0) = \begin{pmatrix} -k_1 & \gamma_2 & -\beta_1 S^0 & -\beta_2 S^0 & -\beta_3 S^0 & -\beta_4 S^0 & \omega \\ \nu & -k_2 & -(1-\rho)\beta_1 V^0 & -(1-\rho)\beta_2 V^0 & -(1-\rho)\beta_3 V^0 & -(1-\rho)\beta_4 V^0 & 0 \\ 0 & 0 & -k_3 & 0 & 0 & 0 & 0 \\ 0 & 0 & \sigma_1 & -k_4 & 0 & 0 & 0 \\ 0 & 0 & \sigma_2 & \eta_1 & -k_5 & 0 & 0 \\ 0 & 0 & 0 & 0 & \nu_1 & -k_6 & 0 \\ 0 & 0 & 0 & \eta_2 & \nu_2 & \tau & -k_7 \end{pmatrix},$$

where $k_i > 0,\ i = 1,2,\ldots,7$ represent the total outflow rates from the corresponding compartments.
To establish local stability, consider the quadratic Lyapunov function

$$V(E,A,I,Q) = \frac{1}{2}\left(p_1 E^2 + p_2 A^2 + p_3 I^2 + p_4 Q^2\right), \quad p_i > 0.$$

Its time derivative along solutions of the infectious compartments is

$$\dot{V} = p_1 E\frac{dE}{dt} + p_2 A\frac{dA}{dt} + p_3 I\frac{dI}{dt} + p_4 Q\frac{dQ}{dt} = \mathbf{x}^T P J_{\mathscr{I}}\mathbf{x},$$

where $\mathbf{x} = (E,A,I,Q)^T$, $P = \mathrm{diag}(p_1,p_2,p_3,p_4)$, and $J_{\mathscr{I}}$ is the infectious submatrix of $J(\mathscr{E}^0)$. By the Gershgorin Circle Theorem [59, 60], all eigenvalues of $J_{\mathscr{I}}$ have negative real parts if the natural outflow rates k_i dominate the infection terms $\beta_i S^0$ and $(1-\rho)\beta_i V^0$, which is equivalent to $\mathscr{R}_e < 1$. Therefore, $\dot{V} < 0$ for all nonzero $\mathbf{x}$, and the DFE is locally asymptotically stable. Conversely, if $\mathscr{R}_e > 1$, at least one eigenvalue becomes positive, rendering $\mathscr{E}^0$ unstable. ■

4. the endemic equilibrium point (EEP)
At the endemic equilibrium, the disease remains present in the population and all state variables of system (1) are non-negative. In particular, the existence of a strictly positive infected class I^{**} guarantees a unique endemic equilibrium whenever $\mathbb{R}_0 > 1$. The endemic equilibrium is therefore given by

$$\mathscr{E}^1 = \left(S^{**},V^{**},E^{**},A^{**},I^{**},Q^{**},R^{**},\right) \in \mathbb{R}^7_+.$$

This equilibrium satisfies the population balance relation

$$\frac{dN(t)}{dt} = \sum_{X\in\{S,V,E,A,I,Q,R\}} \frac{dX(t)}{dt}.$$

Owing to the analytical complexity of system (1), all equilibrium components are expressed as functions of the steady-state infected population I^{**}.

$$\begin{aligned}
S^{**} &= \frac{k_3k_4k_5\big((1-\rho_{h0})+k_2\big)}{\lambda^{**}(\eta_1\sigma_1+k_4\sigma_2)\big((1-\rho)(1+\nu)+k_2\big)}I^{**},\\
V^{**} &= \frac{k_3k_4k_5\,\nu\big((1-\rho_{h0})+k_2\big)}{\lambda^{**}(\eta_1\sigma_1+k_4\sigma_2)\big((1-\rho)+k_2\big)\big((1-\rho)(1+\nu)+k_2\big)}I^{**},\\
E^{**} &= \frac{k_4k_5}{\eta_1\sigma_1+k_4\sigma_2}I^{**},\\
A^{**} &= \frac{\sigma_1k_5}{\eta_1\sigma_1+k_4\sigma_2}I^{**},\\
Q^{**} &= \frac{\nu_1}{k_6}I^{**},\\
R^{**} &= \frac{\sigma_1k_5k_6+(\nu_1+\nu_2k_6)(\eta_1\sigma_1+k_4\sigma_2)}{k_6(\eta_1\sigma_1+k_4\sigma_2)}I^{**}.
\end{aligned} \tag{3}$$

Theorem 4. *The endemic equilibrium point, denoted by $\mathscr{E}^1$, will be globally asymptotically stable in the feasible region if the basic reproduction number, $\mathbb{R}_0 > 1$.*

Proof. To establish the global asymptotic stability of the endemic equilibrium $\mathscr{E}^1 = (S^{**},V^{**},E^{**},A^{**},I^{**},Q^{**},R^{**})$, we apply the Lyapunov–LaSalle invariance principle. Owing to the nonlinear and highly coupled structure of the model, we therefore construct a weighted quadratic Lyapunov function with appropriately chosen positive coefficients. Define

$$\begin{aligned}
\mathscr{V} = {}& \frac{c_1}{2}(S-S^{**})^2 + \frac{c_2}{2}(V-V^{**})^2 + \frac{c_3}{2}(E-E^{**})^2 + \frac{c_4}{2}(A-A^{**})^2 + \frac{c_5}{2}(I-I^{**})^2 + \frac{c_6}{2}(Q-Q^{**})^2\\
&+ \frac{c_7}{2}(R-R^{**})^2,
\end{aligned} \tag{4}$$

where $c_i > 0$, $i = 1,\ldots,7$, are constant weighting coefficients. Clearly, $\mathscr{V}$ is positive definite with respect to $\mathscr{E}^1$ and radially unbounded in the feasible region Ω.
Differentiating $\mathscr{V}$ along the solutions of the system yields

$$\dot{\mathscr{V}} = \sum_{i=1}^{7} c_i (x_i - x_i^{**}) \dot{x}_i,$$

where $x_i \in \{S, V, E, A, I, Q, R\}$. Substituting the model equations and using the equilibrium relations satisfied at $\mathscr{E}^1$, $\dot{\mathscr{V}}$ can be rearranged as

$$\dot{\mathscr{V}} = -\sum_{i=1}^{7} c_i k_i (x_i - x_i^{**})^2 + \mathscr{C},$$

where $k_i > 0$ denote the total removal rates from each compartment and $\mathscr{C}$ collects the cross-product terms generated by infection and progression processes.
The constants c_i are chosen such that all cross terms in $\mathscr{C}$ vanish. In particular, one may select

$$c_3 = \frac{c_1 S^{**}}{E^{**}}, \quad c_4 = \frac{c_3 \sigma_1}{\eta_1 + \eta_2 + \mu}, \quad c_5 = \frac{c_3 \sigma_2}{\nu_1 + \nu_2 + \delta + \mu},$$

with c_6 and c_7 defined analogously according to the balance of flows at $\mathscr{E}^1$. With these choices, the derivative satisfies

$$\dot{\mathscr{V}} \leq 0 \quad \text{for all } (S, V, E, A, I, Q, R) \in \Omega,$$

and $\dot{\mathscr{V}} = 0$ if and only if

$$S = S^{**},\ V = V^{**},\ E = E^{**},\ A = A^{**},\ I = I^{**},\ Q = Q^{**},\ R = R^{**}.$$

Hence, the largest invariant set contained in

$$\left\{(S, V, E, A, I, Q, R) \in \Omega : \dot{\mathscr{V}} = 0\right\}$$

is the singleton $\{\mathscr{E}^1\}$. By the Lyapunov–LaSalle Invariance Principle, every solution initiating in Ω converges to $\mathscr{E}^1$ as $t \to \infty$ whenever $\mathbb{R}_0 > 1$. Therefore, the endemic equilibrium $\mathscr{E}^1$ is globally asymptotically stable. ■

3.3. Global asymptotic stability analysis

The global stability of the DFE within $\Omega \in \mathbb{R}_+^7$ is obtained by denoting the system (1) by

$$\frac{dX(t)}{dt} = F(X(t), Y(t)),$$
$$\frac{dY(t)}{dt} = G(X(t), Y(t)), G(X(t), 0) = 0$$

where $X(t) = (S(t), V(t), R(t))$ comprises of the uninfected sub-populations and $Y(t) = (E(t), A(t), I(t), Q(t))$ comprises of the infected and infectious sub-populations. The global asymptotic stability of the DFE is guaranteed if $\mathbb{R}_0 < 1$ and the two conditions below hold:

- Condition I: For $\frac{dX(t)}{dt} = F(X(t), 0)$, $X^* = (S^0, V^0, E^0, A^0, I^0, Q^0, R^0)$ is GAS, and
- Condition II: $G(X(t), Y(t)) = AY(t) - G^*(X(t), Y(t))$, $G^*(X(t), Y(t)) \geq 0 \ \forall\ (X(t), Y(t)) \in \mathbb{R}_+^7$, where $A = D_Y G(X^*, 0)$ and $\mathbb{R}_+^7$ is the invariant region of the model equations.

Theorem 5. *Let $\mathscr{R}_0$ denote the basic reproduction number of system (1). The disease-free equilibrium*

$$\mathscr{E}^0 = (S^0, V^0, E^0, A^0, I^0, Q^0, R^0) = \left(\frac{\alpha k_2}{k_1 k_2 - \nu\omega}, \frac{\nu\alpha}{k_1 k_2 - \nu\omega}, 0, 0, 0, 0, 0 \right) \in \mathbb{R}^7_+.$$

is globally asymptotically stable (GAS) whenever $\mathscr{R}_0 < 1$.

Proof. Write the system (1) in the form

$$\frac{dX}{dt} = F(X), \quad \frac{dY}{dt} = G(X,Y),$$

where

$$X = (S, V, R)^T, \quad Y = (E, A, I, Q)^T.$$

Stability of the uninfected subsystem is obtained by setting $Y = 0$ in system (1). This implies that

$$\begin{aligned} \frac{dS}{dt} &= \alpha + \omega R - (\nu + \mu)S, \\ \frac{dV}{dt} &= \nu S - \mu V, \\ \frac{dR}{dt} &= -(\omega + \mu)R. \end{aligned}$$

This subsystem is linear and positively invariant in $\mathbb{R}^3_+$. Solving explicitly gives

$$\lim_{t\to\infty} S(t) = S^0, \quad \lim_{t\to\infty} V(t) = V^0, \quad \lim_{t\to\infty} R(t) = 0,$$

where S^0 and V^0 are as given above. Hence, the uninfected subsystem is GAS.

For the infected subsystem, we define $Y = (E, A, I, Q)^T$. The infected subsystem can be written as

$$\frac{dY}{dt} = DY - G^*(X,Y),$$

where

$$D = \begin{pmatrix} -k_3 & 0 & 0 & 0 \\ \sigma_1 & -k_4 & 0 & 0 \\ \sigma_2 & \eta_1 & -k_5 & 0 \\ 0 & 0 & \nu_1 & -k_6 \end{pmatrix},$$

and

$$G^*(X,Y) = \begin{pmatrix} \lambda S + (1-\rho)\lambda V \\ 0 \\ 0 \\ 0 \end{pmatrix} \geq 0,$$

Notice that D is an M-matrix (negative diagonals, non-negative off-diagonals) and $G^*(X,Y) \geq 0$ in $\mathbb{R}^7_+$.

Hence, by the Castillo–Chavez theorem [61, 62], if $\mathscr{R}_0 < 1$, the uninfected subsystem dominates the infection terms in $G^*(X,Y)$, which ensures that all trajectories of $Y(t)$ decay to zero. Therefore, $\mathscr{E}^0$ is globally asymptotically stable in $\mathbb{R}^7_+$ whenever $\mathscr{R}_0 < 1$. ■

3.4. Sensitivity analysis

The sensitivity index (SI) of all the model parameters of system (1) is obtained by calculating the normalized forward sensitivity index for each parameter of $\mathbb{R}_0$ with respect to a parameter Ψ [1, 2, 12].

Definition 6. The normalized forward sensitivity index of $\mathbb{R}_0$, with respect to a parameter Ψ, is defined by

$$S_{\Psi}^{\mathbb{R}_0} = \frac{\partial \mathbb{R}_0}{\partial \Psi} \times \frac{\Psi}{\mathbb{R}_0}. \tag{5}$$

Equation (5) is used to obtain the expression for the SI of each of the parameters of $\mathbb{R}_0$. For instance, the SI of $\mathbb{R}_0$ with respect to π is given as

$$S_{\nu}^{\mathbb{R}_0} = \frac{\partial \mathbb{R}_0}{\partial \nu} \times \frac{\nu}{\mathbb{R}_0} \approx -\frac{28}{100}$$

Hence, the sensitivity indices for each parameter of $\mathbb{R}_0$ can be derived from eq. (5) and the parameter values in Table 3.

Table 2. Sensitivity index of $\mathbb{R}_0$

Parameter	Sign	SI
α	+ve	1.0000
δ	-ve	0.0107
γ_1	+ve	0.2751
μ	-ve	1.0004
ν	-ve	0.2753
τ	-ve	0.0131
β_1	+ve	0.0966
β_2	+ve	0.2713
β_3	+ve	0.6175
β_4	+ve	0.0147
η_1	+ve	0.0063
η_2	-ve	0.2773
ν_1	-ve	0.5972
ν_2	-ve	0.0110
σ_1	-ve	0.0583
σ_2	-ve	0.0381

Table 2 indicates that the sensitivity indices of the parameters α, γ_1, β_1, β_2, β_3, β_4, η_1 are positive, reflecting their direct role in enhancing disease transmission and persistence. In particular, increases in the effective contact or transmission rates (β_1,β_2,β_3,β_4) lead to a higher number of secondary infections, thereby increasing the basic reproduction number $\mathbb{R}_0$. Similarly, an increase in the recruitment rate α or the progression-related parameter γ_1 contributes to sustaining transmission within the population. Conversely, the parameters δ, μ, ν, τ, η_2, ν_1, ν_2, σ_1, σ_2 have negative sensitivity indices, indicating their suppressive effect on disease transmission or their role in shortening the infectious period. For instance, the vaccination rate ν has a negative sensitivity index because increasing vaccination reduces the pool of susceptible individuals available for infection. By moving individuals from the susceptible class into a protected or partially protected class, vaccination disrupts transmission chains and consequently reduces $\mathbb{R}_0$.

3.4. Optimal control problem (OCP) formulation

The system of COVID-19 dynamics given in system (1) is extended into an OCP by introducing four time-dependent variables $u_i(t), i = 1,2,3$, where:

1. $u_1(t) =$ prevention, including travel restrictions and personal protection;

2. $u_2(t)$ = continuous vaccination of susceptible individuals; and
3. $u_3(t)$ = testing, isolation, and treatment of infected individuals.

The description of each of the three control variables is given below:

(i) The control variable $0 \leq u_1(t) \leq 1$ represents preventive efforts, which include personal protection measures and travel restrictions to minimize exposure to COVID-19. The probability of COVID-19 transmission from exposed, asymptomatic, symptomatic, or quarantined individuals to susceptible individuals under $u_1(t)$ is reduced by $(1-u_1(t))$. Therefore, the modified transmission rate is represented as $P^c_{\beta_i} = (1-u_1(t))\beta_i S(t)$, for $i = 1,2,3,4$.

(ii) The control variable $0 \leq u_2(t) \leq 1$ accounts for the continuous vaccination of susceptible individuals. Vaccination reduces the susceptible class by migrating them to the vaccinated class. The vaccination rate of susceptible individuals is represented by $P^c_v = \nu u_2(t)S(t)$.

(iii) The control variable $0 \leq u_3(t) \leq 1$ captures the efforts to test, isolate, and treat infected individuals. Testing and isolation aim to detect and quarantine infected individuals early, reducing their contact with the susceptible population. The term $u_3(t)$ modifies the rate of progression of infected individuals to the quarantined class, and this rate is represented as $P^c_I = u_3(t)I(t)$.

Our aim is to minimize the following cost functional

$$J(u_1,u_2,u_3) = \int_0^{t_f} (\kappa_1 E(t) + \kappa_2 A(t) + \kappa_3 I(t) + \kappa_4 Q(t))\, dt + \frac{1}{2}\sum_{i=1}^{3} \omega_i u_i^2(t), \tag{6}$$

subject to the non-linear ordinary differential equations below:

$$\begin{aligned}
\frac{dS}{dt} &= \alpha + \gamma V + \omega R - (1-u_1)\lambda S - \nu u_2 S - \mu S,\\
\frac{dV}{dt} &= \nu u_2 S - (1-\rho)\lambda V - \gamma V - \mu V,\\
\frac{dE}{dt} &= (1-u_1)\lambda S + (1-\rho)\lambda V - \sigma_1 E - \sigma_2 E - \mu E,\\
\frac{dA}{dt} &= \sigma_1 E - \eta_1 u_3 A - \eta_2 A - \mu A,\\
\frac{dI}{dt} &= \sigma_2 E + \eta_1 u_3 A - \nu_1 I - \nu_2 I - \delta I - \mu I,\\
\frac{dQ}{dt} &= \nu_1 I - \tau Q - \delta Q - \mu Q,\\
\frac{dR}{dt} &= \eta_2 A + \nu_2 I + \tau Q - \omega R - \mu R,
\end{aligned} \tag{7}$$

and the initial conditions in eq. (2). It should be noted that t_f stands for the maximum or final time for the implementation of the control strategies. The balancing weight constants for exposed, asymptomatic, infected, and quarantined individuals are represented by $\kappa_i > 0$, $i = 1,2,3,4$ by respectively. The terms $\frac{1}{2}\omega_i u_i^2(t)$, $i = 1,2,3,4$ represent the costs of implementing prevention measures, continuous vaccination, testing and isolation of infected individuals, and controlling reinfection of recovered individuals, respectively. Thus, the main aim is to evaluate the optimal controls $u_1^*(t)$, $u_2^*(t)$, and $u_3^*(t)$ such that

$$J(u_1^*(t),u_2^*(t),u_3^*(t),) = \min_{\Phi} J(u_1(t),u_2(t),u_3(t)),$$

where

$$\Phi = \{u_i(t) : u_i(t) \in [0,1],\ 0 \leq t \leq t_f,\ i = 1,2,3\}$$

are Lebesgue measurable functions.

3.5. Existence of optimal control problem

To obtain an optimal solution, we first obtain the Lagrangian and Hamiltonian functions for the OCP consisting of the objective functional eq. (6) and the state system (7). Hence, the Lagrangian of the OCP is defined as follows:

$$\mathscr{L}(x,\xi,t) = (\kappa_1 E(t) + \kappa_2 A(t) + \kappa_3 I(t) + \kappa_4 Q(t)) + \frac{1}{2}\sum_{i=1}^{3} \omega_i u_i^2(t). \tag{8}$$

The Hamiltonian function is formulated by introducing the adjoint variables $\lambda_j(t)$, $j \in \{S,V,E,A,I,Q,R\}$ corresponding to the model's state variables, defined as:

$$\mathscr{H} = \mathscr{L}(x,\xi,t) + \sum_{j=1}^{7} \lambda_i \cdot \dot{X}_i(t), \tag{9}$$

where $\dot{X}_j(t)$ denotes the derivatives of the state variables with respect to time, representing their dynamics as defined in the control model.

Theorem 7. *The optimal control problem given by (6) - (7) with the initial conditions at $t = 0$, if there exists $(u_1^*(t), u_2^*(t), u_3^*(t)) \in \Phi$ such that*

$$J(u_1^*(t), u_2^*(t), u_3^*(t)) = \min_{u_1(t),u_2(t),u_3(t)\in\Phi} J(u_1(t), u_2(t), u_3(t)), \tag{10}$$

then an optimal control exists.

Proof. To prove the results in Theorem 7, the following properties will be established:

i The control set is convex and closed.
ii Non-negative solutions of the system (7) exist and are bounded.
iii The Lagrangian eq. (8) is convex with respect to the control.
iv There exist constants $n_1, n_2 > 0$ and $n_3 > 1$ such that the Lagrangian eq. (8) is bounded below by the quantity of the form

$$n_1 \|\xi\|^{n_3/2} - n_2.$$

(i) Since Φ contains all its limit points, the control set Φ is closed. Hence, given $\lambda \in [0,1]$ and any two arbitrary points $\mathbf{x}, \mathbf{y} \in \Phi$, where $\mathbf{x} = (\mathbf{x_1}, \mathbf{x_2}, \mathbf{x_3})$ and $\mathbf{y} = (\mathbf{y_1}, \mathbf{y_2}, \mathbf{y_3})$, we have:

$$\lambda \mathbf{x_i} + (1-\lambda)\mathbf{y_i} \in \Phi \quad \text{for } i = 1,2,3.$$

The convexity property of the control set eq. (10) is satisfied.

ii The optimal control problem eq. (6) subject to eq. (7) and the initial conditions (2) can be written in the compact form

$$\frac{d\mathscr{W}}{dt} = \mathscr{D}(\sqcap)\mathscr{W} + \mathscr{G}(\sqcap, \mathscr{W}), \tag{11}$$

where

$$\mathscr{W}(t) = \begin{pmatrix} S(t) \\ V(t) \\ E(t) \\ A(t) \\ I(t) \\ Q(t) \\ R(t) \end{pmatrix}, \quad \sqcap(t) = (u_1(t), u_2(t), u_3(t))^T.$$

The linear part is given by

$$\mathscr{D}(\sqcap) = \begin{pmatrix} -\nu u_2 - \mu & \gamma & 0 & 0 & 0 & 0 & \omega \\ \nu u_2 & -k_2 & 0 & 0 & 0 & 0 & 0 \\ 0 & 0 & -k_3 & 0 & 0 & 0 & 0 \\ 0 & 0 & \sigma_1 & -(\eta_1 u_3 + \eta_2 + \mu) & 0 & 0 & 0 \\ 0 & 0 & \sigma_2 & \eta_1 u_3 & -k_5 & 0 & 0 \\ 0 & 0 & 0 & 0 & \nu_1 & -k_6 & 0 \\ 0 & 0 & 0 & \eta_2 & \nu_2 & \tau & -k_7 \end{pmatrix}, \tag{12}$$

and the nonlinear part by

$$\mathscr{G}(\sqcap, \mathscr{W}) = \begin{pmatrix} \alpha - (1-u_1)\lambda S \\ -(1-\rho)\lambda V \\ (1-u_1)\lambda S + (1-\rho)\lambda V \\ 0 \\ 0 \\ 0 \\ 0 \end{pmatrix}. \tag{13}$$

The functions $\mathscr{D}(\sqcap)\mathscr{W}$ and $\mathscr{G}(\sqcap, \mathscr{W})$ are continuous and bounded on $\mathbb{R}^7_+ \times [0, t_f]$, and satisfy a Lipschitz condition:

$$\left|\mathscr{H}(\mathscr{W}_1) - \mathscr{H}(\mathscr{W}_2)\right| \leq C \sum_{i=1}^{7} \left|\mathscr{W}_{1i} - \mathscr{W}_{2i}\right|, \tag{14}$$

where $\mathscr{H}(\mathscr{W}) = \mathscr{D}(\sqcap)\mathscr{W} + \mathscr{G}(\sqcap, \mathscr{W})$ and $C > 0$ is independent of $\mathscr{W}$. Therefore, there exists a unique, non-negative and bounded solution $\mathscr{W}(t) \in \mathbb{R}^7_+$ for each Lebesgue measurable control $u_i(t)$, $i = 1, 2, 3$.
Since the integrand of the cost functional eq. (6) is convex in u_i and the control set is bounded and closed, Filippov's existence theorem [63, 64] guarantees the existence of an optimal control

$$(u_1^*, u_2^*, u_3^*) \in L^\infty([0, t_f], [0, 1]^3),$$

that minimizes eq. (6) subject to eq. (7). Furthermore, from eq. (11), we have

$$|\mathscr{H}(\mathscr{W}_1) - \mathscr{H}(\mathscr{W}_2)| \leq P |\mathscr{W}_1 - \mathscr{W}_2|, \tag{15}$$

where $P = \sum_{i=1}^{7} J_i + |M| < \infty$. This shows that $\mathscr{H}(\mathscr{W})$ is uniformly Lipschitz continuous, hence the state system has a unique solution.
Consequently, the Lagrangian is decomposed as

$$\begin{aligned} \mathscr{L}(x, \xi, t) &= \mathscr{L}_1(x, t) + \mathscr{L}_2(\xi, t), \\ \mathscr{L}_1(x, t) &= \kappa_1 E + \kappa_2 A + \kappa_3 I + \kappa_4 Q, \\ \mathscr{L}_2(\xi, t) &= \frac{1}{2} \sum_{i=1}^{3} \omega_i u_i^2(t). \end{aligned}$$

Clearly, $\mathscr{L}_2(\xi, t)$ is convex in u, and satisfies

$$\mathscr{L}(x, \xi, t) \geq \frac{1}{2} \sum_{i=1}^{3} \omega_i u_i^2(t) \geq n_1 \Big(\sum_{i=1}^{3} \|\xi_i(t)\|^2 \Big)^{n_3/2} - n_2,$$

for positive constants n_1, n_2, n_3. Therefore, by Filippov's theorem, an optimal control exists.

■

3.5. Optimal Control Chracterization

The Hamiltonian $(\mathscr{H})$ and the optimality system are derived by applying PMP to the OCPs, which transforms equations eqs. (6) and (7) into a problem of minimizing, pointwise, the Hamiltonian function $\mathscr{H}$ with respect to the optimal control u_i, $i = 1,2,3$. Thus, the Hamiltonian function is as follows:

$$\begin{aligned}\mathscr{H} = {} & \kappa_1 E + \kappa_2 A + \kappa_3 I + \kappa_4 Q + \frac{1}{2}\sum_{i=1}^{3} \omega_i u_i^2 \\ & + \lambda_S\Big(\alpha + \gamma V + \omega R - (1-u_1)\lambda S - \nu u_2 S - \mu S\Big) \\ & + \lambda_V\Big(\nu u_2 S - (1-\rho)\lambda V - \gamma V - \mu V\Big) \\ & + \lambda_E\Big((1-u_1)\lambda S + (1-\rho)\lambda V - \sigma_1 E - \sigma_2 E - \mu E\Big) \\ & + \lambda_A\Big(\sigma_1 E - \eta_1 u_3 A - \eta_2 A - \mu A\Big) \\ & + \lambda_I\Big(\sigma_2 E + \eta_1 u_3 A - \nu_1 I - \nu_2 I - \delta I - \mu I\Big) \\ & + \lambda_Q\Big(\nu_1 I - \tau Q - \delta Q - \mu Q\Big) \\ & + \lambda_R\Big(\eta_2 A + \nu_2 I + \tau Q - \omega R - \mu R\Big),\end{aligned} \tag{16}$$

where λ_j for $j = (S,V,E,A,I,Q,R)$ represents the adjoint variables for the corresponding state variables.

Theorem 8. *Given the optimal control u_i for $i = 1,2,3$ and solutions of the state variables S^*, V^*, E^*, A^*, I^*, Q^*, R^*, there exist adjoint variables λ_j for $j = S,V,E,A,I,Q,R$ satisfying*

$$\frac{d\lambda_j}{dt} = -\frac{\partial \mathscr{H}}{\partial j}$$

with the corresponding transversality conditions

$$\lambda_j(t_f) = 0, \quad j = (S,V,E,A,I,Q,R, \tag{17}$$

and the characterization of the control variables is given by:

$$\begin{aligned} u_1^*(t) &= \min\left\{1, \max\left\{0, \frac{(\lambda_E - \lambda_S)S(\beta_1 E + \beta_2 A + \beta_3 I + \beta_4 Q)}{\omega_1}\right\}\right\}, \\ u_2^*(t) &= \min\left\{1, \max\left\{0, \frac{\nu S(\lambda_S - \lambda_V)}{\omega_2}\right\}\right\}, \\ u_3^*(t) &= \min\left\{1, \max\left\{0, \frac{\eta_1 A(\lambda_A - \lambda_I)}{\omega_3}\right\}\right\}. \end{aligned}$$

that minimizes $J(u_1^*(t), u_2^*(t), u_3^*(t))$ over Φ.

Proof. Differentiating the Hamiltonian eq. (16) with respect to each state variable yields

$$\begin{aligned} \frac{d\lambda_S}{dt} &= -\frac{\partial \mathscr{H}}{\partial S} = \lambda_S\big((1-u_1)\lambda + \nu u_2 + \mu\big) - \lambda_E(1-u_1)\lambda - \lambda_V \nu u_2, \\ \frac{d\lambda_V}{dt} &= -\frac{\partial \mathscr{H}}{\partial V} = \lambda_V\big((1-\rho)\lambda + \gamma + \mu\big) - \lambda_S\gamma - \lambda_E(1-\rho)\lambda, \end{aligned}$$

$$\begin{aligned}
\frac{d\lambda_E}{dt} &= -\frac{\partial \mathscr{H}}{\partial E} = -\kappa_1 + \lambda_S(1-u_1)\beta_1 S + \lambda_V(1-\rho)\beta_1 V - \lambda_E[(1-u_1)\beta_1 S + (1-\rho)\beta_1 V - (\sigma_1+\sigma_2 \\
&\quad +\mu)] - \lambda_A\sigma_1 - \lambda_I\sigma_2, \\
\frac{d\lambda_A}{dt} &= -\frac{\partial \mathscr{H}}{\partial A} = -\kappa_2 + \lambda_S(1-u_1)\beta_2 S + \lambda_V(1-\rho)\beta_2 V - \lambda_E[(1-u_1)\beta_2 S + (1-\rho)\beta_2 V] + \lambda_A(\eta_1 u_3 \\
&\quad +\eta_2+\mu) - \lambda_I\eta_1 u_3 - \lambda_R\eta_2, \\
\frac{d\lambda_I}{dt} &= -\frac{\partial \mathscr{H}}{\partial I} = -\kappa_3 + \lambda_S(1-u_1)\beta_3 S + \lambda_V(1-\rho)\beta_3 V - \lambda_E[(1-u_1)\beta_3 S + (1-\rho)\beta_3 V] + \lambda_I(\nu_1 \\
&\quad +\nu_2+\delta+\mu) - \lambda_Q\nu_1 u_3 - \lambda_R\nu_2, \\
\frac{d\lambda_Q}{dt} &= -\frac{\partial \mathscr{H}}{\partial Q} = -\kappa_4 + \lambda_S(1-u_1)\beta_4 S + \lambda_V(1-\rho)\beta_4 V - \lambda_E[(1-u_1)\beta_4 S + (1-\rho)\beta_4 V] + \lambda_Q(\tau \\
&\quad +\delta+\mu) - \lambda_R\tau, \\
\frac{d\lambda_R}{dt} &= -\frac{\partial \mathscr{H}}{\partial R} = \lambda_R(\omega+\mu) - \lambda_S\omega.
\end{aligned} \tag{18}$$

with the transversality conditions at final time t_f:

$$\lambda_i(t_f) = 0, \quad i = S,V,E,A,I,Q,R.$$

If (x,u) is the optimal solution, then $\frac{\partial \mathscr{H}}{\partial u_1} = \frac{\partial \mathscr{H}}{\partial u_2} = \frac{\partial \mathscr{H}}{\partial u_3} = 0$ at $u_i = u_i^*$

$$\begin{aligned}
\frac{\partial \mathscr{H}}{\partial u_1} &= -\omega_1 u_1 - \lambda_S(A\beta_2 + E\beta_1 + I\beta_3 + Q\beta_4)S + \lambda_E(A\beta_2 + E\beta_1 + I\beta_3 + Q\beta_4)S, \\
\frac{\partial \mathscr{H}}{\partial u_2} &= S\nu\lambda_S - S\nu\lambda_V - \omega_2 u_2, \\
\frac{\partial \mathscr{H}}{\partial u_3} &= \eta_1 I\lambda_I - \eta_1 I\lambda_Q - \omega_3 u_3.
\end{aligned}$$

Hence,

$$\begin{aligned}
u_1^* &= \frac{(\lambda_E - \lambda_S)(A\beta_2 + E\beta_1 + I\beta_3 + Q\beta_4)S}{\omega_1}, \\
u_2^* &= \frac{S\nu(\lambda_S - \lambda_V)}{\omega_2}, \\
u_3^* &= \frac{\eta_1 A(\lambda_A - \lambda_I) + \nu_1 I(\lambda_I - \lambda_Q)}{\omega_3}.
\end{aligned} \tag{19}$$

By the definition of standard control and using the bounds on u_i^*, we obtain

$$\psi_i^* = \begin{cases} 0 \; if \; \vartheta_i^* \le 0, \\ \vartheta_i^* \; if \; 0 < \vartheta_i^* < 1, \\ 1 \; if \; \vartheta_i^* \ge 0, \end{cases}$$

where $i = 1,2,3$ and

$$\vartheta_1 = \frac{(\lambda_E - \lambda_S)(A\beta_2 + E\beta_1 + I\beta_3 + Q\beta_4)S}{\omega_1}$$

Hence, the control for all forms of prevention including travel restrictions, u_1, is given in compact form as

$$u_1^*(t) = \min\{1, \max\{0, \vartheta_1\}\}.$$

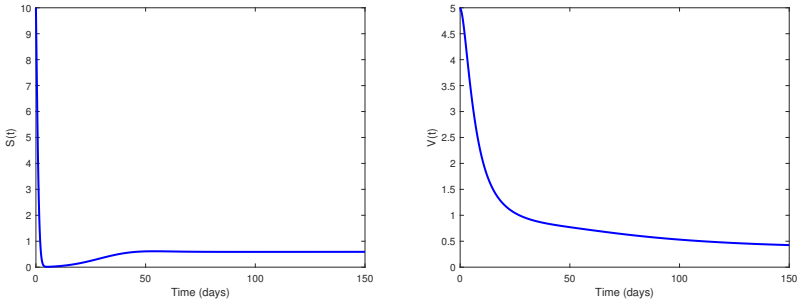

(a) Susceptible Humans **(b)** Vaccinated Humans

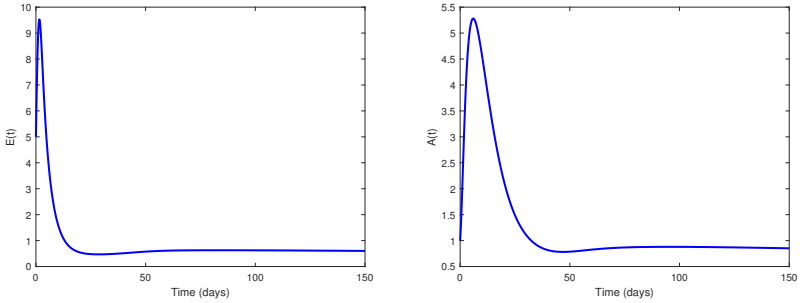

(c) Exposed Humans **(d)** Asymptomatic Infected Humans

Figure 2. Evolution of $S(t)$, $V(t)$, $E(t)$ and $A(t)$ Subpopulations

Similarly,

$$\vartheta_2 = \frac{S\nu(\lambda_S - \lambda_V)}{\omega_2}.$$

Thus, the control for continuous vaccination of susceptible individuals, u_2 is

$$u_2^*(t) = \min\{1, \max\{0, \vartheta_2\}\},$$

and

$$\vartheta_3 = \frac{\eta_1 A(\lambda_A - \lambda_I)}{\omega_3}.$$

Therefore, the compact form of the control for testing, isolation and treatment, u_3, can be written in compact form as

$$u_3^*(t) = \min\{1, \max\{0, \vartheta_3\}\}.$$

■

4. Numerical Results

This section provides the simulation results of the proposed COVID-19 model for both the autonomous and non-autonomous systems, with and without control measures, to demonstrate the model's dynamic behavior. The numerical simulations are performed using MATLAB with the `ode45` solver. Table 3 defines the parameter values and their sources. The initial conditions, in millions, are given by:

$$(S_0, V_0, E_0, A_0, I_0, Q_0, \mathbb{R}_0) = (10, 5, 5, 1, 1, 0, 0).$$

Table 3. Parameter Values

Parameter	Numerical Value	Source
α	0.00005	[65]
μ	0.00005	[1]
ω	0.01762	[49]
β_1	0.05	[66]
β_2	0.1	[67]
β_3	0.3	[67]
β_4	0.001	Assumed
ν	$[0,1]$	Assumed
γ	0.1	[68]
σ_1	0.17	[69]
σ_2	0.15	[54]
η_1	0.05	Assumed
η_2	0.071	[54]
ν_1	0.2	[1]
ν_2	0.0036	[70]
δ	0.003	[71]
τ	0.025	[54]

4.1. Autonomous system

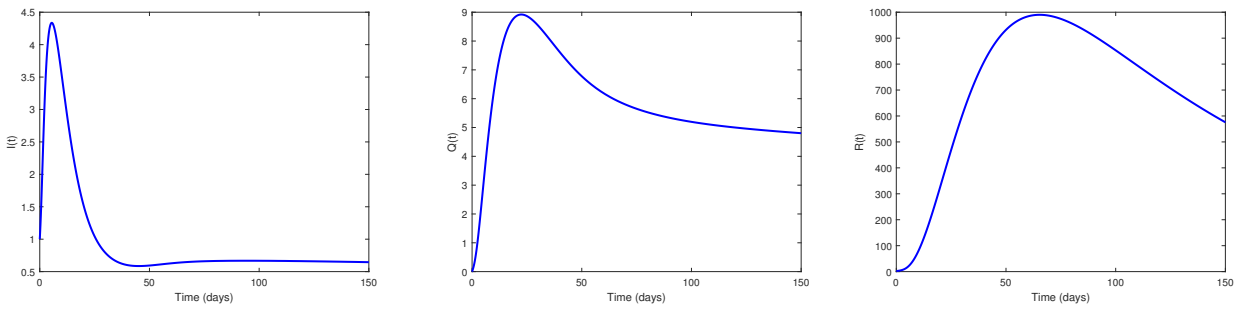

(a) Infected Humans **(b)** Quarantined Humans **(c)** Recovered Humans

Figure 3. Evolution of $I(t)$, $Q(t)$, and $R(t)$ Subpopulations

The calculated value of $\mathbb{R}_0$ of the system (1) is approximately $\mathbb{R}_0 = 1.1724$ using the values of the parameters in Table 3. Figures 2 and 3 show the results of the numerical simulation of each model compartment of system (1) over a period of 150 days. Figures 2a and 2b show a rapid decrease in the number of susceptible and vaccinated individuals. This is largely due to the progression of individuals from these compartment to the exposed class. Figure 2c indicates that the exposed population increases in the early days and later decreases as individuals progress to the asymptomatic infected class. The asymptomatic infected population experienced a slight increase in the first few days and later begins to decrease rapidly until a near steady state is attained after about 150 days (See Figure 2d). The number of individuals infected with COVID-19 increases rapidly in the early days. This class later begins to decrease due to the progression to the quarantined and recovered classes as shown in Figure 3a. This leads to an increase in the number of individuals quarantined compartment in the first few days, as shown in Figure 3b. The population then decreases as a result of the decline in the number of infected individuals. Consequently, there is a rapid increase in the number of recovered individuals, as shown in Figure 3c.

The effects of varying the rate of vaccination, ν, is examined as shown in Figure 4. Figure 4a shows a slight decrease in the humber of susceptible humans while Figure 4b demonstrates that an

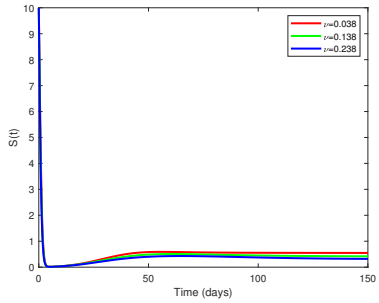

(a) Susceptible Humans

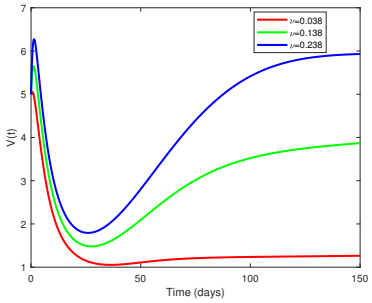

(b) Vaccinated Humans

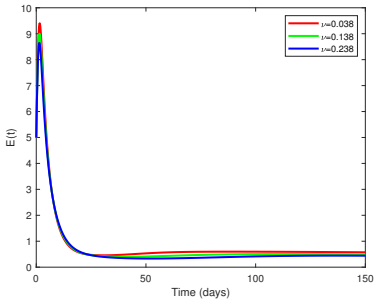

(c) Exposed Humans

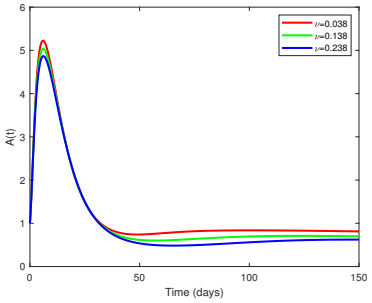

(d) Asymptomatic Infected Humans

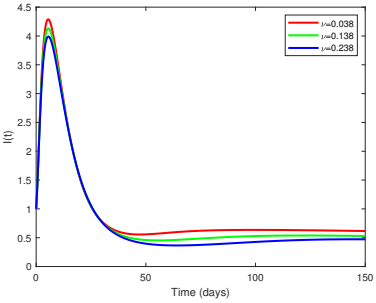

(e) Infected Humans

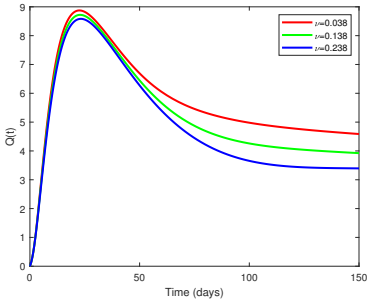

(f) Quarantined Humans

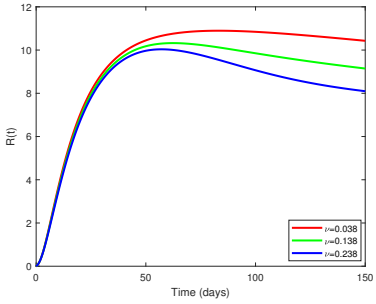

(g) Recovered Humans

Figure 4. Simulation showing the effects of vaccination rate (ν) on $S(t)$, $V(t)$, $E(t)$, $A(t)$, $I(t)$, $Q(t)$ and $R(t)$ Compartments

increase in ν leads to a corresponding increase in the number of individuals vaccinated against COVID-19. Figure 4c to 4f respectively show that as ν_1 increases, there is a corresponding decrease in the population size of each of these classes.

4.2. Non-autonomous system

The iterative forward-backward sweep method (FBSM) combined with the fourth-order Runge-Kutta scheme is employed to solve the sixteen-dimensional optimality system. This system represents a two-point boundary value problem, which consists of the state system (1), the adjoint system (18), and the control characterizations eq. (19) over the given time interval of $[0, 150]$ days. The results are used to determine the optimal control measures that are needed to mitigate the spread of COVID-19 pandemic in an endemic area.

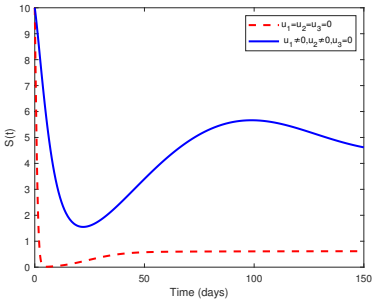

(a) Susceptible Humans

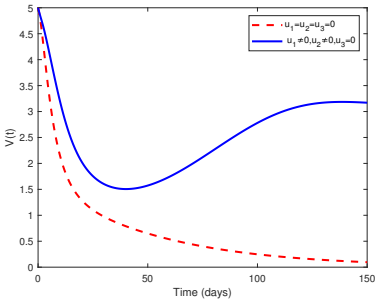

(b) Vaccinated Humans

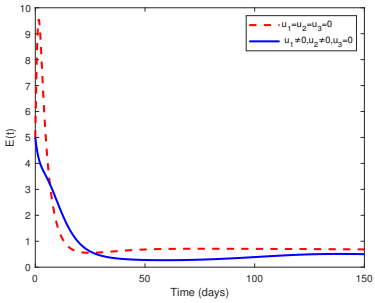

(c) Exposed Humans

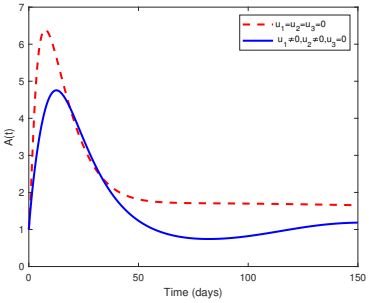

(d) Asymptomatic Infected Humans

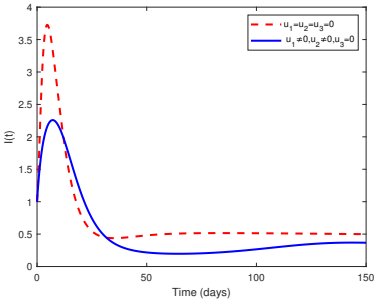

(e) Infected Humans

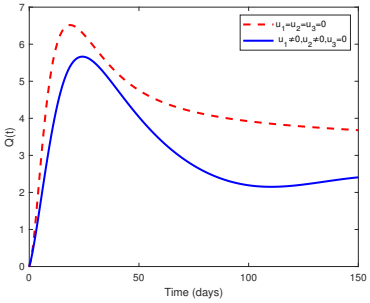

(f) Quarantined Humans

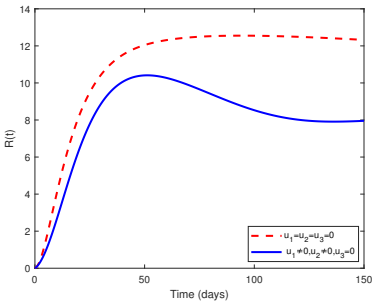

(g) Recovered Humans

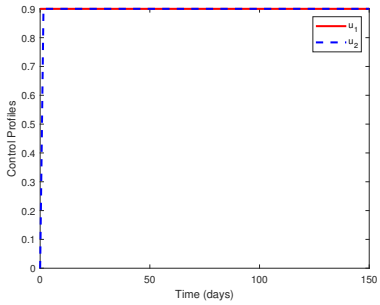

(h) Control Profiles

Figure 5. Effects of strategy A on COVID-19 Population Dynamics

The weight constants κ_i where $i = 1,2,3$ and 4 and u_i where $i = 1,2$, and 3 associated with the objective functional eq. (6), along with the parameter values , are taken as follows: $\kappa_1 = 10$, $\kappa_2 = 15$, $\kappa_3 = 25$, $\kappa_4 = 15$, $\omega_1 = 250$, $\omega_2 = 200$ and $\omega_3 = 125$. These weight are taken theoretically mainly for the numerical solution of the proposed OCP.

Different combinations of the optimal control strategies are examined in order to optimize the objective functional eq. (6). The strategies are:

- strategy A: a combination of optimal prevention, including travel restrictions and personal protection and continuous vaccination of susceptible individuals.(i.e. $u_1(t)$ and $u_2(t)$ with $u_3(t) = 0$);
- strategy B: a combination of optimal prevention, including travel restrictions and personal protection and testing, isolation, and treatment of infected individuals. (i.e. $u_1(t)$ and $u_3(t)$ with $u_2(t) = 0$);
- strategy C: a combination of optimal continuous vaccination of susceptible individuals and test-

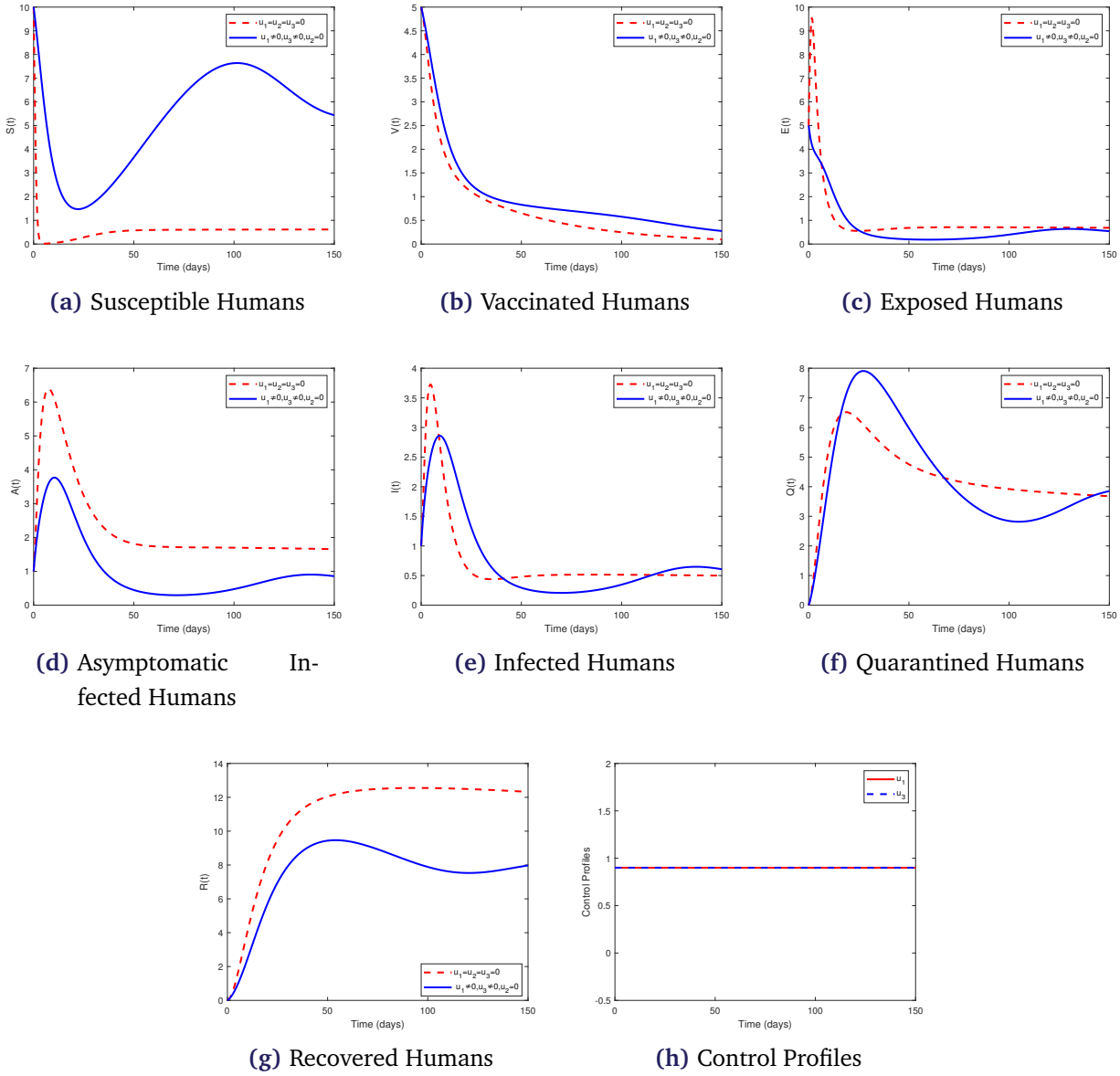

(a) Susceptible Humans **(b)** Vaccinated Humans **(c)** Exposed Humans

(d) Asymptomatic Infected Humans **(e)** Infected Humans **(f)** Quarantined Humans

(g) Recovered Humans **(h)** Control Profiles

Figure 6. Effects of strategy B on COVID-19 Population Dynamics

ing, isolation, and treatment of infected individuals(i.e. $u_2(t)$ and $u_3(t)$ with $u_1(t) = 0$) and

- strategy D: a combination of optimal prevention, including travel restrictions and personal protection, continuous vaccination of susceptible individuals and testing, isolation, and treatment of infected individuals. (i.e. $u_1(t), u_2(t)$ and $u_3(t)$).
- strategy A: a combination of optimal prevention, including travel restrictions and personal protection and continuous vaccination of susceptible individuals.(i.e. $u_1(t)$ and $u_2(t)$ with $u_3(t) = 0$) The first strategy involves a combination of the first two control measures, i.e., optimal prevention (including travel restrictions) and continuous vaccination ($u_1(t) \neq 0$, $u_2(t) \neq 0$, and $u_3(t) = 0$). Figures 5a and 5b show the effects of these two control measures, which rapidly increase the population of susceptible and vaccinated individuals compared to the case without control. The sizes of the exposed, asymptomatic, infected, quarantined, and recovered populations decrease compared to the uncontrolled scenario due to the implementation of this strategy,

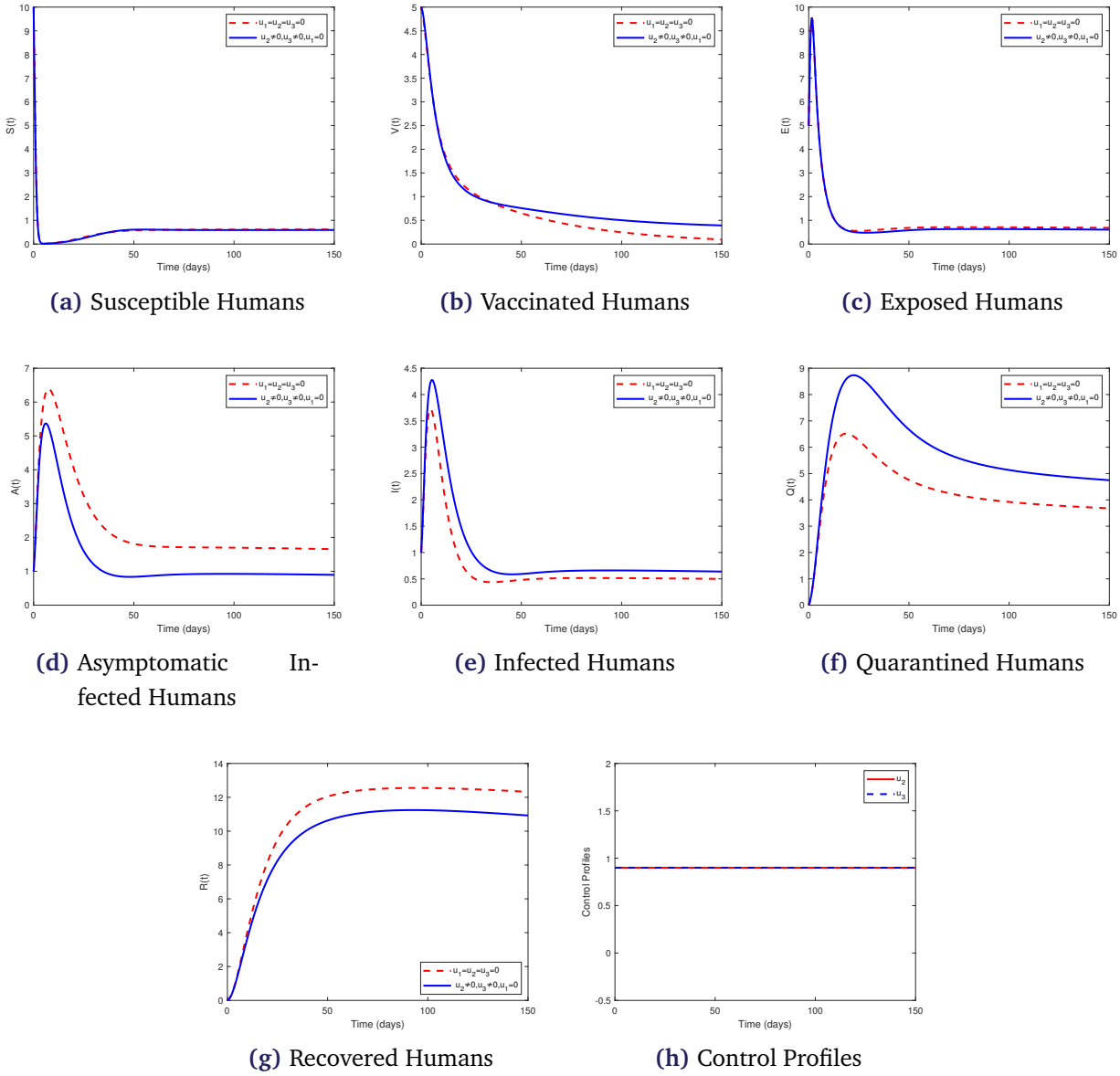

(a) Susceptible Humans **(b)** Vaccinated Humans **(c)** Exposed Humans

(d) Asymptomatic Infected Humans **(e)** Infected Humans **(f)** Quarantined Humans

(g) Recovered Humans **(h)** Control Profiles

Figure 7. Effects of strategy C on COVID-19 Population Dynamics

as shown in Figure 5e to 5c. Figure 5h illustrates the control profile, showing how these two control measures should be implemented effectively. Thus, the graphical results of Strategy A indicate that the implementation of the two control measures can significantly minimize the spread of COVID-19.

- strategy B: a combination of optimal prevention, including travel restrictions and personal protection and testing, isolation, and treatment of infected individuals(i.e. $u_1(t) and u_3(t)$ with $u_2(t) = 0$)
  This strategy combines optimal prevention (including travel restrictions and personal protection), as well as testing, isolation, and treatment of infected individuals, i.e., ($u_1(t) \neq 0$, $u_3(t) \neq 0$, and $u_2(t) = 0$). Figure 6a shows a rapid increase in the population of susceptible individuals. This is as a result of the rapid decrease in the number of infected individuals within the same period, as shown in Figure 6e. Figure 6b indicates that the implementation of this strategy slightly in-

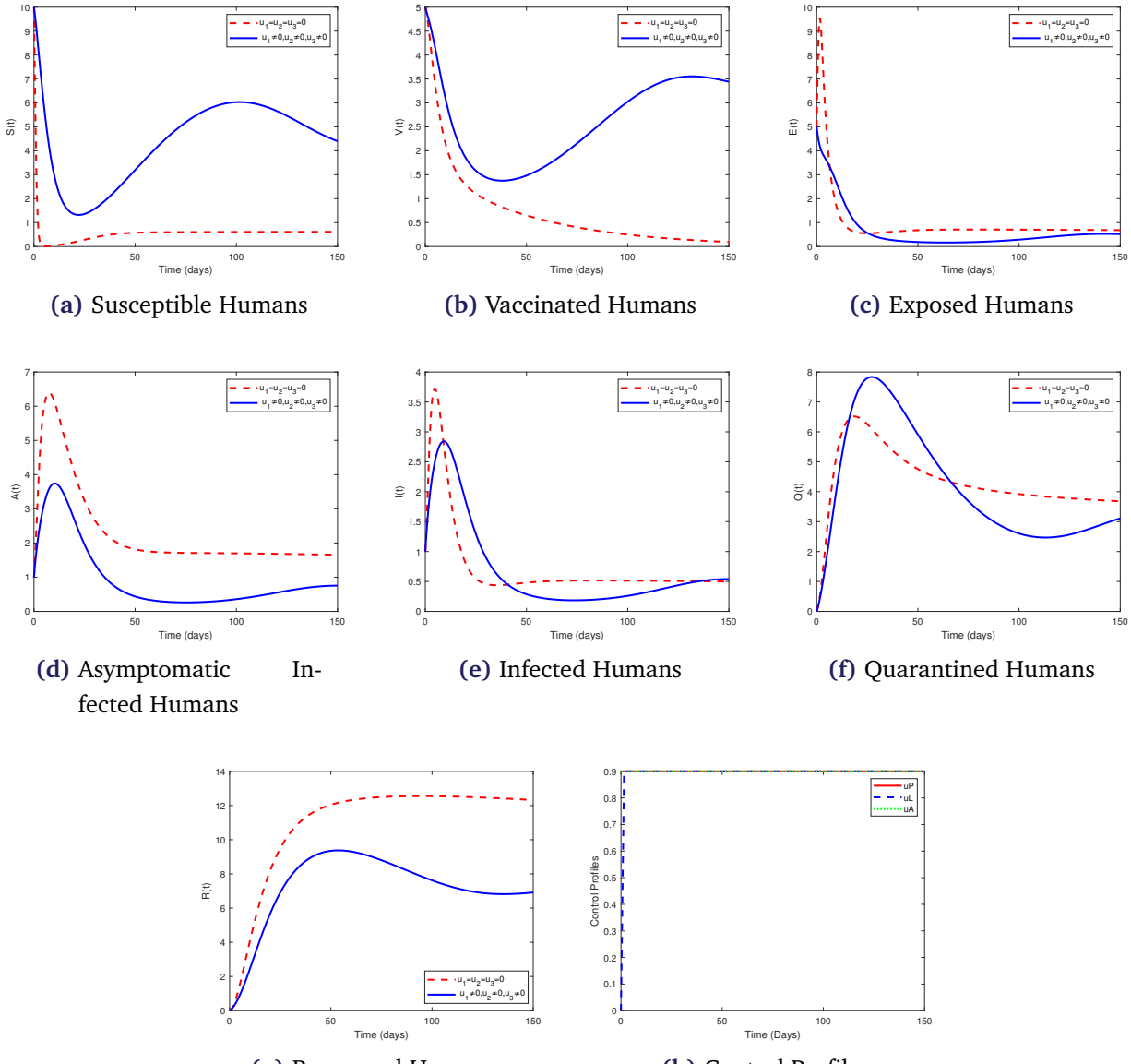

(a) Susceptible Humans **(b)** Vaccinated Humans **(c)** Exposed Humans

(d) Asymptomatic Infected Humans **(e)** Infected Humans **(f)** Quarantined Humans

(g) Recovered Humans **(h)** Control Profiles

Figure 8. Effects of strategy D on COVID-19 Population Dynamics

creases the vaccinated class. Furthermore, Figures 6c and 6d show a decrease in the number of exposed and asymptomatic individuals compared to the case without control. Figure 6f depicts an increase in the number of quarantined individuals. Thereafter, this population decreases due to the reduction in the number of infected individuals. Similarly, Figure 6g shows a decrease in the number of individuals who recover from COVID-19. Figure 6h provides the control profiles illustrating how these two control measures should be implemented. Thus, Strategy B proves to be highly effective in minimizing the spread of COVID-19.

- strategy C: a combination of optimal continuous vaccination of susceptible individuals and testing, isolation, and treatment of infected individuals(i.e. $u_2(t)$ and $u_3(t)$ with $u_1(t) = 0$)
  Strategy C involves a combination of continuous vaccination of susceptible individuals and testing, isolation, and treatment of infected individuals, i.e., ($u_2(t) \neq 0$, $u_3(t) \neq 0$, and $u_1(t) = 0$). The implementation of this strategy has no significant effect on the susceptible class (See Figure 7a).

While Figure 7b reveal that the vaccinated class increases slightly, Figure 7c indicate no significant change in the population of exposed individuals. Furthermore, Figure 7d shows an increase asymptomatic populations when compared to the case without control. Figure 7e shows a small increase in the number of infected individuals compared to the case without control. Figures 7f and 7g depict rapid increases in the number of quarantined and recovered individuals. Figure 7h provides the control profiles indicating that the two control measures should be implemented at the maximum levels throughout the intervention period. Thus, strategy C proves to be highly effective in minimizing the spread of the disease.

- strategy D: a combination of optimal prevention, including travel restrictions and personal protection, continuous vaccination of susceptible individuals and testing, isolation, and treatment of infected individuals(i.e. $u_1(t)$, $u_2(t)$ and $u_3(t)$)
  Figure 8 shows the dynamics of the system under the combination of all the control measures, i.e., optimal prevention (including travel restrictions and personal protection), continuous vaccination of susceptible individuals, and testing, isolation, and treatment of infected individuals $u_1(t), u_2(t),$ and $u_3(t)$. As shown in Figure 8a, there is a significant increase in the number of susceptible individuals when all these control measures are fully implemented. Figure 8b shows a rapid increase in the number of vaccinated individuals compared to the case without control. Figure 8c indicates a decrease in the exposed population, leading to a significant reduction in the infected population (see Figures 8d and 8e). In addition, Figures 8e and 8f show that the quarantined and infected populations increases at the initial stage but later decreases when compared to the case without control. Figure 8g shows a significant decrease in the number of individuals who recover from COVID-19. Figure 8h indicate that the three control measures are to be implemented at the maximum levels throughout the intervention period. Thus, the combination of all the control measures proves to be the most effective strategy in minimizing the spread of COVID-19.

5. Conclusion

An autonomous system consisting of seven mutually exclusive classes is proposed and analyzed. The fundamental properties of the model solutions are examined to establish its positivity and well-posedness. The disease-free equilibrium point of the model is shown to be LAS when $\mathscr{R}_0 < 1$ and unstable when $\mathscr{R}_0 > 1$. A sensitivity analysis is conducted to assess the relative impact of various model parameters on the transmission dynamics of COVID-19. In particular, the influence of the vaccination rate, ν, on the disease spread is evaluated. The findings indicate that increasing the vaccination rate significantly reduces the number of asymptomatic, infected, and quarantined individuals. Based on the findings from the sensitivity analysis, the model is extended to a non-autonomous system by introducing three different control variables: prevention, including travel restrictions and personal protection; continuous vaccination of susceptible individuals; and testing, isolation, and treatment of infected individuals. Pontryagin's maximum principle and optimal control theory are used to analyze the OCP. The effects of the four different control strategies each involving at least two of the control variables are investigated on the transmission dynamics of the disease. The numerical simulations established a distinct hierarchy of effectiveness among the control strategies, demonstrating that while all dual-control approaches (A, B, C) contributed to reducing transmission, the integrated triple-control Strategy D provided markedly superior suppression of the epidemic, underscoring the critical advantage of a comprehensive, combined intervention approach.

Supplementary Information

Author Contributions. **Ayodeji Sunday Afolabi:** Conceptualization, Software, Validation, Writing—Review and Editing, Supervision, Project Administration. **Abdulwahab Ridwan:** Methodology, Formal Analysis, Data Curation, Writing—Original Draft Preparation, Visualization. **Both Authors:** Funding Acquisition. All authors

read and approved the final manuscript.

Acknowledgements. The authors sincerely appreciate the valuable comments and constructive suggestions provided by the reviewers.

Funding. This research did not obtain financial backing from any public, commercial or non-profit funding organizations.

Conflict of interest. The author declares that he has no conflicts of interest to report regarding the present study.

Data availability. Not applicable.

References

[1] Yusuf TT, Abidemi A, Afolabi AS, Dansu EJ. Optimal Control of the Coronavirus Pandemic with Impacts of Implemented Control Measures. Journal of the Nigerian Society of Physical Sciences. 2022;4(1):88-98. doi:10.46481/jnsps.2022.414.

[2] Abioye AI, Peter OJ, Ogunseye HA, Oguntolu FA, Oshinubi K, Ibrahim AA, et al. Mathematical model of COVID-19 in Nigeria with optimal control. Results in Physics. 2021;28:104598. doi:10.1016/j.rinp.2021.104598.

[3] Joshua EE, Akpan ET, Inyang UG. Computational Nonlinear Dynamics: Analysis and Assessment in Optimal Control of COVID-19 in Akwa Ibom State, Nigeria. Journal of Advances in Mathematics and Computer Science. 2024;39(1):1-19. doi:10.9734/jamcs/2024/v39i11858.

[4] Okuonghae D, Omame A. Analysis of a mathematical model for COVID-19 population dynamics in Lagos, Nigeria. Chaos, Solitons and Fractals. 2020;139:110032. doi:10.1016/j.chaos.2020.110032.

[5] World Health Organization. COVID-19 epidemiological update – 15 March 2024. Https://WwwWhoInt/Publications/M/Item/Covid-19-Epidemiological-Update-15-March-2024. 2024;(March):2-3.

[6] Ayoola TA, Kolawole MK, Popoola AO. Effects of Acceptance of Enlightenment on COVID-19 Transmission using Homotopy Perturbation Method. Jambura Journal of Biomathematics. 2022 dec;3(2):39-48. doi:10.34312/jjbm.v3i2.15798.

[7] Akanni JO, Abidemi A, Fatmawati F, Chukwu CW. A Non-linear Fractional Model for Analyzing the Impact of Vaccination on the Dynamics of COVID-19 in Indonesia. Jambura Journal of Biomathematics. 2025;6(2):109-28. doi:10.37905/jjbm.v6i2.30383.

[8] Sihaloho RSBR, Nasution H. Dynamic analysis of SEIR model for Covid-19 spread in Medan. Jambura Journal of Biomathematics. 2022 dec;3(2):68-72. doi:10.34312/jjbm.v3i2.16878.

[9] Putri NQ, Sianturi P, Sumarno H. Mathematical model of Dynamics of Covid-19 Transmission in Response to Reinfection. Jambura Journal of Biomathematics. 2023 apr;4(1):15-22. doi:10.34312/jjbm.v4i1.18394.

[10] Kamalia PZ, Aldila D. Epidemic Dynamics with Nonlinear Incidence Considering Vaccination Effectiveness. Jambura Journal of Biomathematics. 2025;6(3):222-33. doi:10.37905/jjbm.v6i3.33815.

[11] Acuña-Zegarra MA, Díaz-Infante S, Baca-Carrasco D, Olmos-Liceaga D. COVID-19 optimal vaccination policies: A modeling study on efficacy, natural and vaccine-induced immunity responses. Mathematical Biosciences. 2021;337:108614. doi:10.1016/j.mbs.2021.108614.

[12] Adiga A, Dubhashi D, Lewis B, Marathe M, Venkatramanan S, Vullikanti A. Mathematical Models for COVID-19 Pandemic: A Comparative Analysis. Journal of the Indian Institute of Science. 2020;100(4):793-807. doi:10.1007/s41745-020-00200-6.

[13] Djidjou-Demasse R, Michalakis Y, Choisy M, Sofonea MT, Alizon S. Optimal COVID-19 epidemic control until vaccine deployment. medRxiv. 2020:2020.04.02.20049189. doi:10.1101/2020.04.02.20049189.

[14] Gumel AB, Iboi EA, Ngonghala CN, Elbasha EH. A primer on using mathematics to understand COVID-19 dynamics: Modeling, analysis and simulations. Infectious Disease Modelling. 2021;6:148-68. doi:10.1016/j.idm.2020.11.005.

[15] Lü X, wen Hui H, fei Liu F, li Bai Y. Stability and optimal control strategies for a novel epidemic model of COVID-19. Nonlinear Dynamics. 2021;106(2):1491-507. doi:10.1007/s11071-021-06524-x.

[16] Ojo MM, Benson TO, Peter OJ, Goufo EFD. Nonlinear optimal control strategies for a mathematical model of COVID-19 and influenza co-infection. Physica A: Statistical Mechanics and its Applications. 2022;607:128173. doi:10.1016/j.physa.2022.128173.

[17] Omame A, Nwajeri UK, Abbas M, Onyenegecha CP. A fractional order control model for Diabetes and COVID-19 co-dynamics with Mittag-Leffler function. Alexandria Engineering Journal. 2022;61(10):7619-35. doi:10.1016/j.aej.2022.01.012.

[18] Tchoumi SY, Diagne ML, Rwezaura H, Tchuenche JM. Malaria and COVID-19 co-dynamics: A mathematical model and optimal control. Applied Mathematical Modelling. 2021;99:294-327. doi:10.1016/j.apm.2021.06.016.

[19] World Health Organization. COVID-19 epidemiological update – 15 March 2024. Https://WwwWhoInt/Publications/M/Item/Covid-19-Epidemiological-Update-15-March-2024. 2024;(March):2-3.

[20] Adel W, Günerhan H, Nisar KS, Agarwal P, El-Mesady A. Designing a novel fractional order mathematical model for COVID-19 incorporating lockdown measures. Scientific Reports. 2024;14(1):2926. doi:10.1038/s41598-023-50889-5.
[21] Akanni JO, Fatmawati, Ajao S, Asamoah JKK, Abimbade SF. Mathematical model of COVID-19 dynamics in the presence of multiple controls. Quality and Quantity. 2025;59(Suppl 1):261-90. doi:10.1007/s11135-024-01975-x.
[22] Ali M, Imran M, Khan A. Can medication mitigate the need for a strict lock down?: A mathematical study of control strategies for COVID-19 infection. medRxiv. 2020:2020.05.29.20116749. doi:10.1101/2020.05.29.20116749.
[23] Atangana A, İğret Araz S. Mathematical model of COVID-19 spread in Turkey and South Africa: theory, methods, and applications. Advances in Difference Equations. 2020;2020(1):1-89. doi:10.1186/s13662-020-03095-w.
[24] Awasthi A. A mathematical model for transmission dynamics of COVID-19 infection. European Physical Journal Plus. 2023;138(3):285. doi:10.1140/epjp/s13360-023-03866-w.
[25] Burch E, Khan SA, Stone J, Asgharzadeh A, Dawe J, Ward Z, et al. Early mathematical models of COVID-19 vaccination in high-income countries: a systematic review. Public Health. 2024;236:207-15. doi:10.1016/j.puhe.2024.07.029.
[26] Chinebu TI, Okonkwo CU. Modeling the Optimal Control of the Transmission Dynamics of COVID-19 Infection with Quarantine and Isolation. Global Scientific Journal (GSJ). 2021;9(2).
[27] Deressa CT, Duressa GF. Modeling and optimal control analysis of transmission dynamics of COVID-19: The case of Ethiopia. Alexandria Engineering Journal. 2021;60(1):719-32. doi:10.1016/j.aej.2020.10.004.
[28] Din A, Li Y, Khan T, Zaman G. Mathematical analysis of spread and control of the novel corona virus (COVID-19) in China. Chaos, Solitons and Fractals. 2020;141:110286. doi:10.1016/j.chaos.2020.110286.
[29] Du SQ, Yuan W. Mathematical modeling of interaction between innate and adaptive immune responses in COVID-19 and implications for viral pathogenesis. Journal of Medical Virology. 2020;92(9):1615-28. doi:10.1002/jmv.25866.
[30] Kucharski AJ, Russell TW, Diamond C, Liu Y, Edmunds J, Funk S, et al. Early dynamics of transmission and control of COVID-19: a mathematical modelling study. The Lancet Infectious Diseases. 2020;20(5):553-8. doi:10.1016/S1473-3099(20)30144-4.
[31] Li T, Guo Y. Modeling and optimal control of mutated COVID-19 (Delta strain) with imperfect vaccination. Chaos, Solitons and Fractals. 2022;156:111825. doi:10.1016/j.chaos.2022.111825.
[32] Manabe H, Manabe T, Honda Y, Kawade Y, Kambayashi D, Manabe Y, et al. Simple mathematical model for predicting COVID-19 outbreaks in Japan based on epidemic waves with a cyclical trend. BMC Infectious Diseases. 2024;24(1):465. doi:10.1186/s12879-024-09354-5.
[33] Mandal M, Jana S, Nandi SK, Khatua A, Adak S, Kar TK. A model based study on the dynamics of COVID-19: Prediction and control. Chaos, Solitons and Fractals. 2020;136:109889. doi:10.1016/j.chaos.2020.109889.
[34] Morato MM, Bastos SB, Cajueiro DO, Normey-Rico JE. An optimal predictive control strategy for COVID-19 (SARS-CoV-2) social distancing policies in Brazil. Annual Reviews in Control. 2020;50:417-31. doi:10.1016/j.arcontrol.2020.07.001.
[35] Nguyen HK. Application of mathematical models to assess the impact of the covid-19 pandemic on logistics businesses and recovery solutions for sustainable development. Mathematics. 2021;9(16):1977. doi:10.3390/math9161977.
[36] Pinto Neto O, Kennedy DM, Reis JC, Wang Y, Brizzi ACB, Zambrano GJ, et al. Mathematical model of COVID-19 intervention scenarios for São Paulo—Brazil. Nature Communications. 2021;12(1):418. doi:10.1038/s41467-020-20687-y.
[37] Sameni R. Mathematical Modeling of Epidemic Diseases; A Case Study of the COVID-19 Coronavirus. arXiv preprint arXiv:200311371. 2020. doi:10.48550/arXiv.2003.11371.
[38] Shen ZH, Chu YM, Khan MA, Muhammad S, Al-Hartomy OA, Higazy M. Mathematical modeling and optimal control of the COVID-19 dynamics. Results in Physics. 2021;31:105028. doi:10.1016/j.rinp.2021.105028.
[39] Stăncioi CM, Ștefan IA, Briciu V, Mureșan V, Clitan I, Abrudean M, et al. Solution for the Mathematical Modeling and Future Prediction of the COVID-19 Pandemic Dynamics. Applied Sciences (Switzerland). 2023;13(13):7971. doi:10.3390/app13137971.
[40] Tsay C, Lejarza F, Stadtherr MA, Baldea M. Modeling, state estimation, and optimal control for the US COVID-19 outbreak. Scientific Reports. 2020;10(1):10711. doi:10.1038/s41598-020-67459-8.
[41] Ullah S, Khan MA. Modeling the impact of non-pharmaceutical interventions on the dynamics of novel coronavirus with optimal control analysis with a case study. Chaos, Solitons and Fractals. 2020;139:110075. doi:10.1016/j.chaos.2020.110075.
[42] Yousefpour A, Jahanshahi H, Bekiros S. Optimal policies for control of the novel coronavirus disease (COVID-19) outbreak. Chaos, Solitons and Fractals. 2020;136:109883. doi:10.1016/j.chaos.2020.109883.
[43] Zhao S, Chen H. Modeling the epidemic dynamics and control of COVID-19 outbreak in China. Quantitative Biology. 2020;8(1):11-9. doi:10.1007/s40484-020-0199-0.
[44] Nana-Kyere S, Okyere E, Ankamah JDG. Compartmental seirw Covid-19 optimal control model. Communications in Mathematical Biology and Neuroscience. 2020;2020:1-30. doi:10.28919/cmbn/4998.
[45] Madubueze CE, Dachollom S, Onwubuya IO. Controlling the Spread of COVID-19: Optimal Control Analysis. Computational and Mathematical Methods in Medicine. 2020;2020. doi:10.1155/2020/6862516.
[46] Yan X, Zou Y. Optimal and sub-optimal quarantine and isolation control in SARS epidemics. Mathematical and

Computer Modelling. 2008;47(1-2):235-45. doi:10.1016/j.mcm.2007.04.003.
[47] Kifle ZS, Lemecha Obsu L. Optimal control analysis of a COVID-19 model. Applied Mathematics in Science and Engineering. 2023;31(1):2173188. doi:10.1080/27690911.2023.2173188.
[48] Omede BI, Odionyenma UB, Ibrahim AA, Bolaji B. Third wave of COVID-19: mathematical model with optimal control strategy for reducing the disease burden in Nigeria. International Journal of Dynamics and Control. 2023;11(1):411-27. doi:10.1007/s40435-022-00982-w.
[49] Khan AA, Ullah S, Amin R. Optimal control analysis of COVID-19 vaccine epidemic model: a case study. European Physical Journal Plus. 2022;137(1):1-25. doi:10.1140/epjp/s13360-022-02365-8.
[50] Butt AIK, Imran M, Chamaleen DBD, Batool S. Optimal control strategies for the reliable and competitive mathematical analysis of Covid-19 pandemic model. Mathematical Methods in the Applied Sciences. 2023;46(2):1528-55. doi:10.1002/mma.8593.
[51] Zamir M, Abdeljawad T, Nadeem F, Wahid A, Yousef A. An optimal control analysis of a COVID-19 model. Alexandria Engineering Journal. 2021;60(3):2875-84. doi:10.1016/j.aej.2021.01.022.
[52] El Bhih A, Benfatah Y, Kouidere A, Rachik M. A discrete mathematical modeling of transmission of Covid-19 pandemic using optimal control. Communications in Mathematical Biology and Neuroscience. 2020;2020:1-23. doi:10.28919/cmbn/4780.
[53] Mondal J, Khajanchi S. Mathematical modeling and optimal intervention strategies of the COVID-19 outbreak. Nonlinear Dynamics. 2022;109(1):177-202. doi:10.1007/s11071-022-07235-7.
[54] Goswami NK, Olaniyi S, Abimbade SF, Chuma FM. A mathematical model for investigating the effect of media awareness programs on the spread of COVID-19 with optimal control. Healthcare Analytics. 2024;5:100300. doi:10.1016/j.health.2024.100300.
[55] Bixler SL, Stefan CP, Jay AN, Rossi FD, Ricks KM, Shoemaker CJ, et al. Exposure Route Influences Disease Severity in the COVID-19 Cynomolgus Macaque Model. Viruses. 2022;14(5):1013. doi:10.3390/v14051013.
[56] Ojo MM, Goufo EFD. Assessing the impact of control interventions and awareness on malaria: A mathematical modeling approach. Communications in Mathematical Biology and Neuroscience. 2021;2021:1-31. doi:10.28919/cmbn/6632.
[57] Chen TM, Rui J, Wang QP, Zhao ZY, Cui JA, Yin L. A mathematical model for simulating the phase-based transmissibility of a novel coronavirus. Infectious Diseases of Poverty. 2020;9(1):18-25. doi:10.1186/s40249-020-00640-3.
[58] World Health Organization (WHO). COVID-19 Weekly Epidemiological Update: Edition 185; 2024. https://www.who.int/publications/m/item/weekly-epidemiological-update-on-covid-19---5-march-2024.
[59] Furtat IB, Others. Generalization of Gershgorin Circle Theorem with Application to Analysis and Design of Control Systems. Avtomatika i telemehanika. 2025;(6):3-23.
[60] Weisstein EW. Gershgorin Circle Theorem; 2003. MathWorld—A Wolfram Web Resource.
[61] Castillo-Chavez C, Thieme HR. Asymptotically autonomous epidemic models. Science. 1994;94(38):1-22.
[62] Castillo-Ramirez A, Magaña-Chavez MG. A Study on the Composition of Elementary Cellular Automata. Advances in Cellular Automata: Volume 1: Theory. 2025:347-73. doi:10.1007/978-3-031-78757-7_12.
[63] Filippov AF. On Certain Questions in the Theory of Optimal Control. Journal of the Society for Industrial and Applied Mathematics Series A Control. 1962;1(1):76-84. doi:10.1137/0301006.
[64] Santos ILD, Silva GN. Filippov's selection theorem and the existence of solutions for optimal control problems in time scales. Computational and Applied Mathematics. 2014;33(1):223-41. doi:10.1007/s40314-013-0057-z.
[65] Hethcote HW. Mathematics of infectious diseases. SIAM Review. 2000;42(4):599-653. doi:10.1137/S0036144500371907.
[66] Qiu X, Nergiz AI, Maraolo AE, Bogoch II, Low N, Cevik M. The role of asymptomatic and pre-symptomatic infection in SARS-CoV-2 transmission—a living systematic review. Clinical Microbiology and Infection. 2021;27(4):511-9. doi:10.1016/j.cmi.2021.01.011.
[67] Zhang C, Zhou C, Xu W, Zheng S, Gao Y, Li P, et al. Transmission risk of asymptomatic SARS-CoV-2 infection: a systematic review and meta-analysis. Infectious Medicine. 2023;2(1):11-8. doi:10.1016/j.imj.2022.12.001.
[68] Rădulescu A, Williams C, Cavanagh K. Management strategies in a SEIR-type model of COVID 19 community spread. Scientific Reports. 2020;10(1):e0244082. doi:10.1038/s41598-020-77628-4.
[69] Wu Y, Kang L, Guo Z, Liu J, Liu M, Liang W. Incubation Period of COVID-19 Caused by Unique SARS-CoV-2 Strains: A Systematic Review and Meta-analysis. JAMA Network Open. 2022;5(8):e2228008. doi:10.1001/jamanetworkopen.2022.28008.
[70] Gebreyohannes LT. Investigating the recovery time from SARS-CoV-2 infection and risk factors among COVID-19 patients: a systematic review and meta analysis of survival analysis. Journal of Microbiology & Experimentation. 2025;13(1):16-25. doi:10.15406/jmen.2025.13.00427.
[71] Ozair M, Hussain T, Hussain M, Awan AU, Baleanu D, Abro KA. A Mathematical and Statistical Estimation of Potential Transmission and Severity of COVID-19: A Combined Study of Romania and Pakistan. BioMed Research International. 2020;2020:2020.08.07.20170039. doi:10.1155/2020/5607236.